ARTICLE NO. 79-0160R

Review of Composite Propellant Burn Rate Modeling

Norman S. Cohen
Norman Cohen Professional Services, Redlands, Calif.

Introductory Overview

THE modeling of solid propellant combustion serves a number of useful purposes in the scheme of propellant development. It strives to represent the combustion process in mathematical terms so that the combustion characteristics of proposed formulations can be predicted, reducing the scope of formulation processing trials. It strives to explain the combustion characteristics which are observed, providing a diagnostic tool to help address anomalous or undesirable combustion behavior. It seeks to distinguish governing mechanisms from those of secondary or little importance, so that chemists and engineers may be guided more productively in the means to overcome combustion limitations and achieve propellant tailoring goals. In a more academic vein, it provides a stimulus and focal point for combustion research to improve our understanding and develop new ideas. The purpose of this paper is to review a class of comprehensive, steady-state combustion models which has been evolving in the course of the 1970's.

Most modern solid propellants are "composite" in the sense that powders (also known as fillers or solids) are included in a polymerized medium. On the scale of the fillers, the combustion is a three-dimensional, unsteady process with a complexity of sequences and interactions. Yet the aggregate propellant sample, which is large compared to a filler particle, burns at a measurable "steady-state" isobaric rate on the macroscopic scale. This fact forms the basis for the statistical averaging concept which is the common denominator of the models to be discussed. Work has emphasized ammonium perchlorate (AP) oxidizer-polymeric fuel binder composites because they have been of greatest general interest over the modeling time period. However, the methodology is adaptable to composites generally, and the more recent work has been addressing energetic powders and binders as well.

The statistical combustion modeling originated with Hermance.[1] Basically, the macroscopic propellant is represented by addressing the behavior of a statistical particle and its environment on the microscopic scale. Assumptions and approximations are made to convert the unsteady three-dimensional process to a steady, one-dimensional model. The principal mechanisms which Hermance put into this framework were a dominant AP-binder interfacial surface reaction, and a single premixed flame sheet in the gas. Subsequently, Hermance included diffusional mixing in his flame model.[2] Whatever the shortcomings of the included mechanisms, the work had a profound influence upon the combustion research community. First, it dealt with the general shape of the burn rate-pressure curve of AP propellants over a broad pressure range, and thereby set standards for models while pointing out several regimes of burning. Second, it provided a vehicle with which to account for detailed observations of the combustion zone, so that modeling could be more complementary to the experimental work. Third, it was shown that parametric studies with such a model could be used to guide continuing research and combustion tailoring efforts. One effort[3] set the stage for the Beckstead-Derr-Price (BDP) model,[4] which furnishes the baseline for this paper.

Experiments performed by the formulators of the BDP model showed no basis in fact for the dominating geometric consequences of the Hermance interfacial reaction scheme. Further, the qualities of AP as a monopropellant oxidizer coupled with the overall fuel richness of the AP composite propellants of interest suggested that a single flame model for the gas phase was inadequate. The contention of a multiple flame structure was at that time supported by prior and contemporary observations. Accordingly, the BDP model was created to correct the shortcomings of the Hermance model, incorporating the updated state of knowledge into the Hermance statistical framework. It was shown that the multiple flame structure was a satisfactory alternative to the interfacial reaction in explaining the shape of the burning rate-pressure curve as well as a number of other combustion properties.[4,5] At this juncture, the model was limited to monomodal AP in hydrocarbon binders. Subsequently, Cohen and co-workers[6-8] and Beckstead[9,10] extended the model to encompass more complicated propellants in the same basic statistical framework. The ability to do this, given a poorer state of detailed knowledge, and the proper method to be used are controversial and unresolved questions.[11] Work by these investigators is continuing.

Glick[12-14] objected to the statistical aspects of the BDP model and, together with Condon,[15] incorporated the BDP multiple flame model into a new statistical formalism. The new formalism purported to correct inconsistencies in the BDP approach, and better represent the time and dimension dependent features of the combustion on the microscopic scale. At the same time, the formalism was derived for a polydisperse powder by incorporating a distribution function[16] and adopting the partition/summation method proposed by Miller et al.[17] Basically, each particle group constitutes a "pseudopropellant"; the propellant is sub-

---

Norman S. Cohen has been performing research and development work in the area of solid propellants and combustion since 1961. Until 1975, he was employed by the Aerojet-General Corp. and Lockheed Propulsion Co. He has been self-employed since that time. He holds the degrees of BAE, MSE, and JD. He is a member of the AIAA Technical Committee on Propellants and Combustion, and of the JANNAF Combustion Working Group. In recent years, he has coordinated several JANNAF workshops on various combustion topics.

Presented as Paper 79-0160 at the AIAA 17th Aerospace Sciences Meeting, New Orleans, La., Jan. 15-17, 1979; submitted Jan. 29, 1979; revision received July 16, 1979.

Index categories: Combustion and Combustor Designs; Fuels and Propellants, Properties of; Solid and Hybrid Rocket Engines.

divided into its component pseudopropellants, and the total behavior is the sum of the parts. The method is referred to as the "petit ensemble" model. The work has arrived at a stage of completion, and a detailed summary has recently been published by Condon and Osborn.[18]

Another offshoot of the statistical modeling is being developed by King.[19] The formalism is more closely related to that of Glick, but is presently limited to monomodal AP propellants. The significant aspect of King's work is the consideration of distributed heat release in the condensed phase and in the diffusion flame, although in a simplified way. More formal models of distributed reactions are being developed by Price et al.[20] and by Caveny[21] as applied to the deflagration of the monopropellant powder ingredients (AP, HMX, and RDX).* These models offer a potentially significant improvement to the composite propellant models because description of the monopropellant deflagration is a necessary part. The present treatment of the monopropellant combustion in the statistical models may be too simplified. These investigations are continuing.

A different approach to statistical analysis has been pursued by Miller and co-workers.[17,22,23] For some time, this group has been accumulating and correlating data on AP particle size distribution effects and how these effects are influenced by other formulation variables. The objective has been to determine an effective particle size function that could be used to predict accurately the burning rate of a proposed formulation. Since the statistical correlations are empirically based, it is not a true modeling effort and will not be reviewed here. However, it is cited because of its more immediate practical value to propellant development. Further, the conclusions regarding the particle size effects can furnish guidance to the extended modeling, and the data base is an excellent source of material for model verifications. Some of this will be touched upon in appropriate portions of the paper.

Two discontinued efforts were those of Flanagan and Oberg,[24] and Sammons.[25,26] The interesting aspect of the former was the use of nonlinear optimization in association with selected burn rate data to deduce values for model input constants considered to be least certain. Other modelers have used this technique in those cases where independent means (theory or measurement) were not available. It is sometimes referred to as model calibration, but can be overdone where there are excessive "floating parameters" in the model. At that stage, it can be argued that the modeling has gotten too far ahead of the experiments, but it does point out areas where experiments ought to be conducted. Sammons incorporated a particle size distribution in the BDP framework, and critiqued the method for calculating the diffusion flame. Glick and Condon subsequently followed up on these ideas. Sammons also postulated a critical particle size below which all of the AP would be consumed in a condensed phase reaction. This concept was not followed by others, but related ideas are contained in the works of King, Price-Boggs-Derr, and Miller et al.

Still another approach to statistical modeling has been published by Strahle.[27] Strahle calculated the statistically probable paths of burning through a packed bed of particles representing a composite propellant. Without the benefit of any particular combustion process, but just from burn-through times and the statistics, he argued that important features of composite propellant burning (such as the particle size effect) can be demonstrated. For purposes of steady-state modeling, it appears that Strahle's view is adequately represented by the averaging methods of Hermance or BDP and their offspring. For nonsteady phenomena, however, Strahle's view may have additional significance.

The paper will concentrate on the modeling efforts of Beckstead, Cohen et al., Glick-Condon, and King. Discussions will be limited to the major equations and the similar or differing ideas and assumptions behind them, organized in terms of the common elements of these models. The reader is referred to the source materials and their authors for derivations and additional details. This author will attempt to assist the reader by providing a common nomenclature and a common or comparable equation format. Thus, equations may appear to be different than in the references, but should be consistent except for typographical errors which will be pointed out to the extent detected. The author apologizes if this causes confusion. All of the equations, as well as a nomenclature list, are in the Appendix. Typical results and comparisons with data will be shown to demonstrate the state-of-the-art and support recommendations for future work.

*HMX—cyclotetramethylene tetranitramine. RDX—cyclotrimethylene trinitramine.

Basic Physical Model

The BDP view of an AP particle and its environment, photographed at an instant of time during burning, is shown in Fig. 1. This general representation has been adopted by the various modelers. AP is both a monopropellant and an oxidizer; the surrounding binder was limited to the inert fuel polymer type. The flame structure consists of a premixed monopropellant flame, a primary diffusion flame involving portions of the AP and binder decomposition products, and a final diffusion flame involving the remaining fuel products plus remaining oxidizing species following the monopropellant combustion. Each of these flames furnishes energy to the surface by conduction. In the case of the AP flame, a one-dimensional heat transfer from a flame sheet is a reasonable approximation. In the case of the diffusion flames, which are columnar in nature, the heat transfer would be three-dimensional but approximations are made to convert the problem to one that is effectively one-dimensional. The contribution of each flame to the surface heating depends upon the multiple flame geometry. These allocations, referred to as "competing flame" effects, are perhaps the key feature of this theory. Two additional energy terms are derived from the surface: the heat of decomposition of the binder (endothermic) and the heat of decomposition of the AP (net exothermic). Heterogeneous surface reactions, the key feature of the Hermance model, are not included. All of the energy terms combine to raise the temperature of the solid from its initial bulk temperature to the surface temperature. A uniform surface temperature is assumed, and thermal properties are taken to be constant average values. The uniform surface temperature is recognized to be a poor assumption, but the limited way that the binder enters into the model renders it of minor importance.

The model focuses upon calculation of the AP surface temperature and upon its burning rate as an Arrhenius function of the surface temperature. The binder is assumed to follow along in accordance with continuity to preserve the propellant formulation. The localized burning rate at the time of the photograph is then the total mass flux divided by the

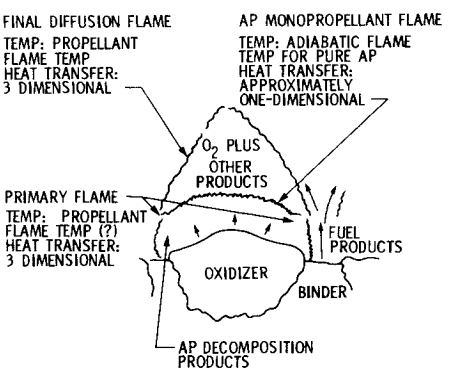

Fig. 1 BDP multiple flame structure (from Ref. 4).

propellant density. Assuming a representative particle at a representative time, this burning rate is the propellant burning rate.

In order to apply continuity and implement some of the constitutive relations in the multiple flame model, something must be known about the surface structure: specifically, exposed ingredient surface areas and characteristic dimensions. It is known that AP particles retain their physical integrity during burning; they do not break up or melt in bulk. It also is known that the particles may protrude above the adjacent binder plane or be recessed ("dished down") into that plane, depending mainly upon the pressure. Thus the surface is bumpy, because of the AP, as illustrated in Fig. 1. The binder is taken to be a plane. The fact that the binder has a surface melt layer, or may char, which could physically interfere with adjacent AP surfaces under certain conditions, is ignored. The surface is given an idealized representation to try to capture the essence of the problem in a tractable way.

The BDP idealization of the surface, again followed by others in general terms, is shown in Fig. 2. This figure depicts the geometric relationship of an AP particle to the burning surface. The propellant is viewed as a packed bed of spherical particles, with binder filling the interstitial spacings. The burning surface is a random planar cut through this packed bed. Half of the particles are cut below their centerline and half above. The statistical average diameter of intersection has been computed [28] to be $\sqrt{2/3}\ D_o$. BDP, Beckstead, and Cohen et al. use this statistical average as the representative particle configuration. In Fig. 2, the intersection is shown above the particle centerline and the intersection diameter is the statistical average D'. The burning surface of the AP is assumed to be a spherical segment. The position of this segment at the time of the photograph is given by how far the AP burns from the top (accounting for ignition delay) in the time that it takes the binder to regress from the top (first exposure of the particle) to the plane of intersection. If the AP is able to outrace the binder, the spherical segment would be dished down rather than up. The same analysis is applied to the particle cut below its centerline, and computation of the surface structure becomes a matter of geometry accounting for both particle groups. The paramater b is a characteristic dimension used in the diffusion flame analysis. Here, then, is one approach for averaging the microscopic time-dependency of the combustion.

Glick-Condon and King have taken a different approach to the time-dependency. They go to the trouble of computing the surface and flame geometries as a function of time for discrete time steps as the plane moves down from the top of the particle to the bottom. There is no statistical average D', but a D' which varies with time. This procedure is illustrated by Fig. 3. The propellant burning rate is not represented by the single photographed state described above, but rather as the time average of an integrated motion picture. The method has intuitive appeal because it more closely resembles the way that propellants actually burn. However, comparisons of results between the two methods show such little difference that the BDP statistical averaging method can be deemed a good approximation after all.

Analyses for Monomodal AP/Inert Binder Propellants

Continuity Relations

The continuity relations are given by Eqs. (1).† Cohen retains the original BDP expression. Glick-Condon have made two changes. First, they argue that m_T should be associated with the total planar surface rather than the total actual surface. They reason that propellant burning rate is with reference to a plane of regression. BDP believed that mass is derived from a total surface, so attempting to extract a single "burning rate" from the behavior of a two-component system in this way requires use of the total actual surface. Hermance used the planar surface, and King concurs; Beckstead follows BDP. The point has not been resolved, and does not make much difference in computed results. Second, and chiefly with multimodal propellants in mind (to be discussed later), the particular α_{ox} need not be the weight fraction as formulated; thus a distinction of α^*_{ox} will be made, although $\alpha^*_{ox} = \alpha_{ox}$ for a propellant having only one particle size. Beckstead, with active binder propellants in mind (to be discussed later), no longer requires the binder to follow the oxidizer to preserve the formulation. Thus, $m_f S_f$ needs to be computed separately. This raises interpretation problems to be discussed later. King also separates the oxidizer and binder components because he feels that forcing the formulation to be preserved here leads to inconsistencies elsewhere in the model.

As noted earlier, the foregoing equations in the King and Glick-Condon models apply at each of several states in the history of the burning particle. Thus, the additional step of Eqs. (1a) is required. A difference in method is apparent. One numerically approximates a time integral, whereas the other averages the mass flows over all of the increments. King discussed a number of possible averaging methods,[19] but reported results based on Eq. (K-1a) while admitting the assumption that each increment is weighted equally even though the times differ. Another problem is raised by the fact that particle burnout generally occurs prior to the time that the binder plane would have reached the bottom of the particle. King refers to this problem as the "end game," and ties it to the averaging question. Glick-Condon exclude the post-consumption increments from the summation with the interpretation that residual material is dispensed with (fills empty pockets, forms a char, or is blown away). An elaborate derivation was presented for the case where the binder plane reaches the bottom prior to particle burnout,[15] but this case was rarely encountered and was removed from the analysis in the interests of computer time. The interpretation would be that oxidizer particles are ejected, and this has not been observed experimentally with inert binders. King includes the post-consumption increments in the averaging as increments having zero mass flow, but expresses uncertainty about it. BDP skirted the issue in an expedient way, and one can accept or reject it. For King or Glick-Condon to resolve this problem in accordance with their approach, it appears necessary to expand the scope of tracking to accommodate more particles. This is not likely to happen because of the effort required and because the credibility of the model and its results does not hinge upon this issue.

All of the models use the same ingredient decomposition relations. See Eqs. (2)

Surface Area Relations

Cohen and Beckstead follow BDP in expressing S_{ox}/S_o, but account for the two sets of particle groups[3,6] [Eqs. (3-5)]. Glick-Condon apply the same geometric analysis, but in general terms to cover the general plane of intersection. The additional step shown in Eq. (GC-3) is given to clarify any confusion that might be caused by typographical errors appearing in Eq. (194) of Ref. 18, and by the choice of total rather than planar surface in that part of the Ref. 18 discussion. If S_{ox} is normalized by S_o rather than S_P Eq. (GC-3) would become identical to Eq. (B-3) for $D' = \sqrt{2/3}\ D_o$ and one overall h ($h_P = h_N$). Thus the analyses are consistent when viewed on a common basis. Glick-Condon also follow the BDP particle ignition delay for purposes of computing d_{ox} and h.

King concurs with Glick-Condon, but with two notable exceptions. First, King does not impose an ignition delay, so the AP has a head start relative to the other models. Consensus would hold this omission to be in error, but it does not seem to have an important bearing upon the results for AP

† All equations will be found in the Appendix.

propellants. Second, King computes S_P as a function of d_f by tracking a burn path through the closest packing particle array in the direction in which the lattice spacing is minimum.[29] He does this to begin to account for the overlapping layers of particles existing in highly loaded propellants, but S_P (and its two components, which are also computed) then becomes a complicated function of oxidizer volume fraction, particle size, and planar location. Since the planar areas are functions of geometry only, they can be generated as external inputs to the iterative portions of the problem. $S_{ox,}$ of course, remains coupled into the problem.

A consequence of the tracking approach is a considerable shift in instantaneous O/F ratio. Glick-Condon assume a constant ζ_{ox} and O/F ratio in the course of tracking to avoid the problem, but King is disturbed about the resulting inconsistency between model geometry and mass flow contributions. This problem seems to be but another consequence of a tracking approach that does not go far enough.

Characteristic Surface Dimension

Cohen follows BDP as to the characteristic surface dimension, b [see Eqs. (C-6) and (C-6a)]. δ is computed by adding all of the D' along the line of intersection, subtracting that total from the total length, and dividing by the total number of particles along the line.[3] This is the width of binder between each particle along that line. Half the width, plus half of D', is the dimension b. An unfortunate typographical error in Ref. 3 caused some controversy[14] over the properties of b which, for some reason, has never gone away.[15, 18, 19] This error showed the term $(\frac{2}{3})^{\frac{1}{2}}$ of Eq. (C-6a) as $(\frac{2}{3})^{\frac{1}{3}}$. In any event, Eq. (C-6a) can compute positive values of δ for ζ_{ox} in excess of 0.9 even though a packed bed of unimodal spheres could never even approach that volume fraction. The reason is that the statistical plane of intersection is away from the equator, so there is room for δ to be squeezed artificially. Clearly, this approach should not be used for monomodal propellants wherein α_{ox} exceeds about 70% (for AP and typical binders). BDP never violated that limitation, and residual criticisms[18] are incorrect.

With multimodal propellants in mind, Glick-Condon adopted a different approach which has since been followed by Beckstead. Essentially, the fractional area of intersection of a plane through a packed bed of spheres is equal to the volume fraction of the spheres.[10,28] Stated another way, the fraction of planar surface occupied by the oxidizer is ζ_{ox}.[14] Applying this principle to the single particle configuration yields Eq. (GC-6). For the statistical average D', Eq. (B-6) results. From Beckstead's point of view, an interesting question is whether the intersection providing the statistical average planar area ratio is consistent with the intersection providing the statistical average D'. Glick[14] has plotted δ/D_o as derived from the two approaches, and the difference is roughly 20% for ζ_{ox} between 0.4 and 0.5. The BDP plane is located a bit further from the equator than the area distribution plane, so there is a small inconsistency in b in the direction of excess fuel. On the other hand, Eq. (GC-6) departs significantly from its premise for the general D' in the course of tracking. The approach takes on more significance for multimodal propellants; for monomodal propellants, it is still constrained by the practical upper limit for ζ_{ox}.

King simply adheres to the geometry existing at each increment of tracking [Eq. (K-6)].

Flame Heights

The diffusion flame analysis has moved in several different directions from the original BDP version. All continue to be based, in one way or another, on the Burke-Schumann analysis[30] of a coaxial Bunsen burner flame as modified by Williams.[31] Referring to Fig. 2, the analogy of the surface to the mouth of a coaxial Bunsen burner is evident. The inner oxidizer jet is of diameter D' and the outer fuel jet extends from D' to b.

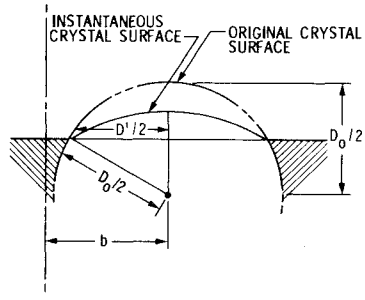

Fig. 2 BDP idealized surface structure (from Ref. 10).

King makes one preliminary change to accommodate the Burke-Schumann assumption that the gas jet velocities are equal. He assumes that the surface areas somehow adjust immediately in the gas phase to meet this requirement. Thus D' adjusts to a new value given by Eq. (K-6a). Implicit in BDP and the other models is that the velocities somehow adjust immediately to a value consistent with m_T/ρ_p to meet this requirement. One artificiality replaces another. It is possible to make too much of this issue because Burke-Schumann do not consider a concaved inner mouthpiece, a displaced inner mouthpiece, or the presence of a competing monopropellant reaction inside the diffusion flame envelope. For this and other reasons, Beckstead and Cohen have essentially abandoned Burke-Schumann model calculations, but have retained a key property of the solution for one limiting condition.

The Burke-Schumann analysis provides a series solution relating the axial and radial coordinates where mixedness is achieved relative to stoichiometry and the flame is located. There are two possible solutions, one where the flame closes over the oxidizer jet and one where it bends over the fuel jet. The BDP model produces the former situation, which is consistent with the physical picture of Fig. 1, but wide swings in O/F ratio possible in other models (or other propellant types) can encounter the latter situation. The BDP model made two important simplifications to reduce computational time. First, it limited the calculation to the center of the oxidizer particle, and assumed a parabolic flame shape, to avoid calculating the entire flame shape. Second, it limited the calculation to the first term of the infinite series. Glick-Condon[18] have shown that this is not a good approximation, although it does provide a closed form expression for the flame height.[3,4] The solution contains a singularity (infinite height) for a value of O/F ratio depending upon the stoichiometry and surface dimensions. The singularity separates the two possible flame bending directions, and is a region where the solution is very sensitive to the underlying parameters.

In further studies of the properties of the solution, Beckstead[9] concluded that the "short flame" limiting condition[3] was reasonably representative of the regime of interest. The expression for the diffusion length becomes Eq. (B-7). The factor A_{fh} converts the parabolic flame into an effective flame sheet for purposes of one-dimensional heat transfer to the surface. It represents that fractional height of the parabola which, as a sheet, transfers the same heat as would the integrated parabola. C_{PD} is a "floating parameter." The expression for η' shown here corrects a typographical error repeated several times in Ref. 3. The expression for x^*_{PD} shown here corrects a manuscript error in Ref. 9, which appears to have confused η' and ν. Since η' remains fairly constant for a given propellant chemistry, and $\phi_l = 3.83$, Beckstead has considered making x^*_{PD} simply a constant times b in his more recent work.

Cohen has taken the same approach, but his expression for x^*_{PD} is Eq. (C-7). The placement of η' in the denominator rather than the numerator is an old error, but of little consequence because η' is fairly constant for a given propellant chemistry. Thus the Cohen value for C_{PD} is different from the

Beckstead value such that Eqs. (B-7) and (C-7) are essentially the same numerically. For AP propellants, the value of C_{PD} used by Cohen[32] has remained unchanged for the decade, so this "floating parameter" has become venerable.

The JANNAF Workshop[11] has not endorsed the Beckstead-Cohen approximations. Consensus prefers further development of the formal Burke-Schumann analysis in the interests of mechanistic accuracy. Glick-Condon and King retain the formal analysis [see Eqs. (GC-7) and (K-7)]. Since King and Glick-Condon anticipate wide variations in O/F ratio, both solution cases are contained. Approximately 10 terms of the series are carried, depending upon numerical convergence criteria. Glick-Condon follow BDP by calculating the peak location, $J_o(\phi_i \xi) = 1$. King, to avoid the singularity, iterates for the point where only 90% of the mixing is achieved.[33] Also, to avoid repetitive case-to-case computations, King[33] has parameterized his solution in the form of look-up correlations by running an extensive set of calculations externally to the combustion model. This approach was endorsed by the Workshop.[11] King also writes ν in terms of mole fractions rather than weight fractions, and accounts for portions used up in subsurface reactions not considered by the other models. King is the only one who accounts for changes in ν in the course of tracking, and who does not use an average flame height.

Glick-Condon follow BDP in expressing $\mathfrak{D}/v$ [Eq. (GC-7e)]. King has a slightly different temperature-dependence for $\mathfrak{D}$, and expresses v in terms of the oxidizer characteristics (with the adjusted area) rather than in terms of m_T. See Eq. (K-7e).

In all of the models, the diffusion flame height is the sum of the mixing height, x^*_{PD} and the kinetics reaction distance x^*_{PF}. King expresses x^*_{PF} from an approximation of Zeldovich premixed flame theory. The others follow BDP, which used an approximation of von Kármán laminar flame theory. See Eqs. (8). All of the models assume that the primary flame achieves the thermochemical flame temperature. King accounts for changes in the thermochemistry with O/F in the course of tracking.

The AP monopropellant flame height is similarly expressed [see Eqs. (9)]. Equation (K-9) differs from Eq. (K-8) because the AP flame is more reasonably approximated by a premixed flame sheet. The more detailed monopropellant models[20,21] are accounting for distributed reactions in calculating the thermal profile in the gas phase.

Beckstead has computed the effect of the final flame to be negligible in the surface energy balance because of its distant location (it is always furthest away, by model definition). Thus he has removed it from the BDP surface energy balance, but keeps it in the model in order to properly compute T_{AP} by accounting for the heat transfer from the final flame to the AP flame. This process is consistent with the physical model, and is also accounted for by Glick-Condon. Cohen agrees that the final flame is negligible, but has retained it in the BDP surface energy balance. The Beckstead approach is the correct one because the final flame serves to heat the AP flame rather than superpose with the AP flame in heating the surface. However, the error is minor so long as the effect of the final flame is small. King omits the final flame completely. The final flame height is given by Eq. (10). Taking the AP flame as the starting point for the mixing region of the final flame is consistent with the physical model. However, the computation of x^*_D may contain a serious conceptual error. It is computed in the same manner as x^*_{PD}, with the same characteristic dimensions, but with an average temperature (between T_{AP} and T_F) replacing T_S and with m_{ox} replacing m_T in Eq. (GC-7e). The characteristic dimensions should not be the same above the surface as they were at the surface. An argument can be made that they are smaller, which could have a significant impact upon high pressure results which are currently in error. The point needs to be re-examined. The omission of a reaction distance for the final flame is of negligible effect.

All of the flame heights are nondimensionalized in accordance with one-dimensional heat transfer analysis in the gas phase, [see Eq. (11)]. King uses m_T for the flames, which results from his area adjustments to achieve uniform gas velocity. Beckstead, Cohen, and Glick-Condon use m_T for the primary flame but m_{ox} for the other flames; although this may be consistent with the physical picture, it is no longer possible to interpret a consistency with the Burke-Schumann requirement of uniform velocity. Beckstead and Cohen avoid the issue to the extent that they evolve away from Burke-Schumann.

Energy Balance

The energy balance as written by BDP is followed by Cohen and Glick-Condon. [See Eq. (C-12)]. The flame terms are in the form of one-dimensional heat transfer analysis from a flame sheet. The superposition of the AP flame and the final flame is considered to be error. Glick-Condon properly feed the energy from the final flame back to the AP flame for purposes of Eq. (9a), but not here. For purposes of Eq. (9a), Eq. (9b) is used. The β_F term is an attempt to partition the AP reactants between the primary flame on the one hand and the sequence of the AP and final flames on the other hand. Since this could not be done in the diffusion analysis, it is done by projecting the flame areas on the planar surface of the AP.[3] The AP and final flames project on the same inner circle; the primary flame projects on the remaining outer annulus. Thus, the partitioning can be interpreted as one based upon geometric zones of energy influence[19] (a quasi two-dimensional effect), but it is meant to be based upon species. This is how the competing flame feature of the model becomes operative.

Beckstead now writes an energy balance for each oxidizer and binder.[10] This is done primarily with active binder propellants in mind, but is applicable to inert binders also. However, all of Beckstead's results (to be shown later) are based upon an earlier version[9] having the single energy balance. In keeping with the present discussion (simple propellants), the simpler version will be used here. The extended version and its problems will be deferred to a later discussion. The simpler version can be written as Eq. (B-12). Beckstead now includes detailed species partitioning in expressing Q'_{AP}. For purposes of the present discussion, it can be obtained from Eqs. (9b) and (12a). All of the other Eq. (12) relations are the same. In this simpler version, $m_f S_f$ is not computed separately but follows the oxidizer to preserve the formulation.

King makes two changes from the BDP approach. First, there is partitioning of surface energy terms to account for more surface processes. The current monopropellant modeling is considering the AP in similar detail.[20] Second, the diffusion flame is taken to release its heat uniformly over the diffusion distance rather than singularly at the flame height. This method approximates distributed reactions, which is also a feature of the current monopropellant work. King also accounts for differences in specific heats, but a constant specific heat version will be shown here to facilitate comparison with the other models. The result is Eq. (K-12). The fraction of AP reacted in subsurface reactions, β_{oxSS}, is determined by integrating the Arrhenius equation in a reactive layer but assuming a nonreactive thermal profile. This error can be corrected by reference to the thin reactive melt layer analysis of Bowyer and Cohen.[34] The reactive layer thermal profile is nearly linear which is quite different from the exponential profile assumed by King. With β_{oxSS} thus defined, β_{fSS} is determined assuming that a stoichiometric amount of fuel reacts with the oxidizer in the subsurface reactions. Subsurface reactions involving both oxidizer and inert binder are not generally accepted. The β_F from the BDP model (but without A_{fh}, may be isolated in King's equation, but the overall competing flame partitioning is seen to be complicated by distributed heat release. Incorporation of the more

comprehensive monopropellant models would complicate this further.

It is has been suggested[11] that the more comprehensive monopropellant models could be incorporated into the composite propellant model framework by parameterizing the monopropellant solutions. This would be analogous to what King has done with the Burke-Schumann model. Thus tables could be called for AP or HMX, etc., as appropriate in the propellant solution procedure. Beckstead[35] has argued that the simplified monopropellant model, as presently contained, is adequate but there is much disagreement.

The foregoing equations are solved by a numerical iteration because surface temperature, surface areas, mass flux, and flame heights are all interdependent.

Extensions to Multimodal and Active Binder Propellants

Glick-Condon

In the Glick-Condon view, there is no such thing as a unimodal propellant. This is, of course, true in the sense that no propellant is made with particles which are literally all of one size. Thus they make a distinction between "monodisperse" (all sizes the same) and "polysperse" (a distribution of sizes about some mean) in referring to any given "particle size" that is incorporated into a propellant. Similarly, the distinction is made for multimodal propellants which are monodisperse or polydisperse. However, this distinction is less significant in multimodal propellants because it boils down to how many particle sizes are to be treated in the model. For a trimodal distribution, Cohen and Beckstead would treat 3 particles whereas Glick – Condon might treat 50. In treating the 50 particles, however, it is as though each were monodisperse. The practical upper limit is computer time. From this standpoint of practicality, Glick-Condon are able to treat many particles because their model is less detailed than King's and because they assume that all particle solutions are uncoupled. Cohen and the current Beckstead models treat few particles because they attempt to couple the solutions in some way; they have found that coupled solutions entail a geometric growth in computer time, whereas uncoupled solutions entail an arithmetic growth or very little growth depending upon method and what assumptions or approximations are made. The Workshop[11] sought, as a reasonable goal, a coupled solution of four particles (monodisperse) with distribution functions applied in some simplified representative way (simulated polydisperse).

Glick-Condon obtain the propellant burning rate by summing the proportional contributions of each size component (each pseudopropellant) to the mass flux. The procedural relation is given by Eq. (GC-14). The heart of the problem is the monomodal model presented previously, which determines the mean state $\dot{m}_{Ti}$ of each size D_i. This is added over all sizes in the mth mode, each component being weighted in accordance with a log-normal size distribution function representing its proportional amount. The log-normal distribution is a very good representation of size distributions incorporated into propellants.[18, 36] Results are then summed over all m modes for the jth oxidizer, each mode weighted in accordance with its fraction of the total solids. For a monomodal AP propellant, $j=1$, $m=1$, and $F_m=1$. Note that a given particle size may properly appear in more than one mode; for example, 10μ may be the mean size of $m=1$ and also a fine component of $m=2$ having a mean of 50μ. Lastly, results are summed over all j oxidizers. In this framework, a different model for a different oxidizer would be reflected in the method of calculating $\dot{m}_{Ti}$. Glick-Condon have not, however, performed any computations for mixed oxidizer propellants.

The remaining task is to define ζ^*_{ox}, or the amount of binder to be allocated to oxidizer in each pseudopropellant. Glick-Condon argue that, considering the manner in which particles are packed and wetted in real propellants, the relation is not simply based on a weight proportion. Further, they argue that the BDP model cannot be used as a guide because it does not describe local binder pocket volumes. One thought might be to apportion based on particle surface area, considering wetting only, and this has been adopted by Beckstead in his current work. Glick-Condon prefer to leave it as a floating parameter particle size dependence. The result is Eq. (GC-15). ζ^*_{ox} replaces ζ_{ox} in all of the constitutive relations for $\dot{m}_{Ti}$. It can be verified that $\zeta^*_{oxi}=\zeta_{oxi}$ for $C_N=3$, which would be the simple weight proportioning. $C_N=2$ corresponds to proportioning based on surface area (current Beckstead). Parametric results for an 87.4% AP/HTPB propellant are shown in Fig. 4. Note that, for $C_N<3$, fine sizes become fuel-rich and coarse sizes become oxidizer-rich. This is taken into account in the mixture ratio and thermochemistry of each size. Note also that it impacts the characteristic dimensions and other size-dependent aspects of the problem. As might be expected, the burning rate of each pseudopropellant is sensitive to the value of C_N (especially for the finer sizes).[14] The propellant burning rate becomes largely a question of the extent to which the finer sizes contribute. In any event, essentially all of the published results are for $C_N=3$, so $\zeta^*_{oxi}=\zeta_{oxi}$ anyway.

Probably the chief criticism of Glick-Condon here is that the gross propellant behavior cannot simply be a summation of uncoupled and noninteracting parts. Secondly, there are implicit violations of formulation continuity because the contributions are not constrained to their proportions as formulated. The interpretation of inactive leftover material leaves something to be desired.

Beckstead and Cohen et al. Methods

Beckstead and Cohen have two model versions, which might be called old version[6,9] and current version.[8,10] In each case, the distinguishing feature is the number of surface temperatures calculated. In the old version, only one surface temperature is calculated. Beckstead superposed up to three contributing diffusion flames (trimodal oxidizer) in a single energy balance. Essentially, Eq. (12) was expanded for three sets of competing flames with formulation continuity preserved completely. The characteristic dimension of each flame was calculated by assuming that the smallest particle is part of a higher density binder as far as the larger particles are concerned, and that the space occupied by larger particles is gone from a shrunken propellant volume as far as the smaller particles are concerned. Equation (B-7) was used to compute each diffusion length. Cohen and Price with Derr calculated a single diffusion flame based upon an average characteristic dimension for bimodal oxidizer. Cohen used the BDP method to calculate an average δ, which is open to question for multimodal packings because the particles are not all lined up as they are in the unimodal array. He then presented a heuristic argument that the characteristic dimension should be based upon this δ and the fine D' because he found that use of an average D' did not give good results. The data then available indicated a dominance of the fines, arguably because the fines more efficiently use up binder (δ becomes very small compared to the coarse D') and the coarse diffusion flame is relatively distant. This trend would also be reflected in Beckstead's model, and runs contrary to Glick's argument for $C_N<3$ (the fines are stoichiometrically starved). Since Cohen-Price-Derr calculated one surface temperature from a single energy balance, formulation continuity was preserved. With respect to surface structure, Cohen-Price-Derr superposed each contribution to S_{ox} according to volume fraction (the size dependence is in t_{ign}, which Beckstead dismissed as having a negligible effect). Although these two models indicate ways of treating bimodal or trimodal oxidizer through averaging and superposition, they are too simple and not physically satisfying. The new versions were aimed

toward mixed oxidizer and active binder propellants, but could be applied to multimodal propellants also. Cohen and Price with Strand have published results from the new version,[8] but Beckstead has not as yet.

The new version continuity relations for a dual-oxidizer active binder propellant are given by Eqs. (B-14) and (C-14). The only difference between the two equations is that Beckstead calculates the planar binder area explicitly, from binder volume fraction, whereas Cohen-Price-Strand constrain the binder area to that remaining after the oxidizer areas are calculated. There is an inconsistency in Beckstead's method because the oxidizer surface is not generally planar. For inert binders, Cohen-Price-Strand preserve continuity as between binder and total oxidizer by replacing the binder term in a fashion analogous to Eq. (C-1). For active binders, they assume that the binder burns with such independence that the binder burning rate (as a monopropellant) can be input directly for r_f. Beckstead calculates a separate surface temperature for the binder, and does not preserve either oxidizer-oxidizer or oxidizer-binder continuities, whether the binder is active or inert. Either way, the binder burning rate is a function of its surface temperature in accordance with Eq. (2b).

Cohen continues to calculate a δ by the BDP method, but now extends it to four particle sizes to accommodate two bimodal oxidizers. His intent was to use the old version model for each bimodal oxidizer, and the new version to couple the two oxidizers. Cohen uses this scheme for mixed nitramine propellants where the diffusion flame is less significant (see later), but does not recommend a four-particle calculation in this way where AP is involved. The equation for δ is cumbersome[8] and will not be reproduced here. Given this δ, b for each oxidizer is one-half the sum of δ and the appropriate D'. Thus there are two sets of multiple flames, one for each oxidizer, requiring two energy balances for two surface temperatures. The Beckstead b for each particle is now given by Eq. (B-6), but requires the proper ζ^*_{ox} in accordance with Glick's approach. Beckstead takes $C_N = 2$ and obtains (by independent derivation) Eq. (B-15), which is consistent with Eq. (GC-15). The ζ^*_{oxi} is used to compute a diffusion flame temperature for each particle. Examples of what happens when this is done for trimodal AP propellants are shown in Fig. 5. The drop in flame temperature is significant and requires the insertion of another floating parameter to adjust the flame height. Cohen-Price-Strand, who do not use this approach, assume that the propellant flame temperature is applicable to both flames. An argument can be made for that assumption in the case of multimodal propellants, but it is not physically consistent or realistic for mixed oxidizer propellants.

The Cohen-Price-Strand energy balance for each oxidizer (or particle, when using this approach for bimodal propellants) is given by Eq. (C-16). The $(m_{ox}S_{ox})$ summation can be related to m_T through Eq. (C-15). For inert binder, it is simply $m_T\ S_o$ times the sum of α_{oxj}. Note that the energy balance and binder are apportioned in accordance with oxidizer mass flow. It is through this, the dependence of diffusion flame height on m_T, and the fact that m_T as computed for $j=1$ must equal that as computed for $j=2$, that the solution is said to be "coupled."

Beckstead's energy balance, following some manipulation and correction of a typographical error, is for each oxidizer (or size) given by Eq. (B-16). For the binder, it is Eq. (B-17). The elaborations stem from the desire to assign species and energy. Portions of the AP and binder go to the primary flame (β_F). A portion of the AP reacts stoichiometrically in the AP flame (β_{AP}). Remaining species go to the final flame. A portion of the primary flame heats the AP (γ), the remainder heats the binder. The assigned proportion is arbitrarily based on A_{fh}, which has a value of $\frac{1}{3}$. If the binder is active, there is another flame term which is treated like the AP flame (but with different kinetics constants). A detailed model of double-base propellant combustion is not used. The portion of binder species which do not go to the primary flame go to the "double-base" flame (β_{DB}). For an active binder, O/F should be thought of in terms of mass flows rather than "oxidizer" and "fuel." It is certainly plausible that fuel species from an active binder can form a primary

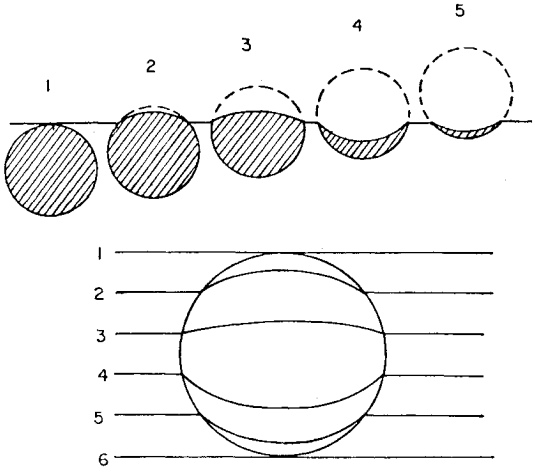

Fig. 3 Birth and consumption of an AP particle as viewed by Glick-Condon (from Ref. 18).

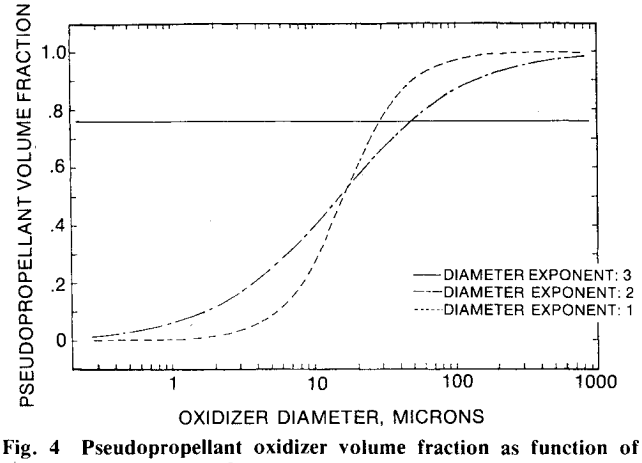

Fig. 4 Pseudopropellant oxidizer volume fraction as function of particle size (from Ref. 18).

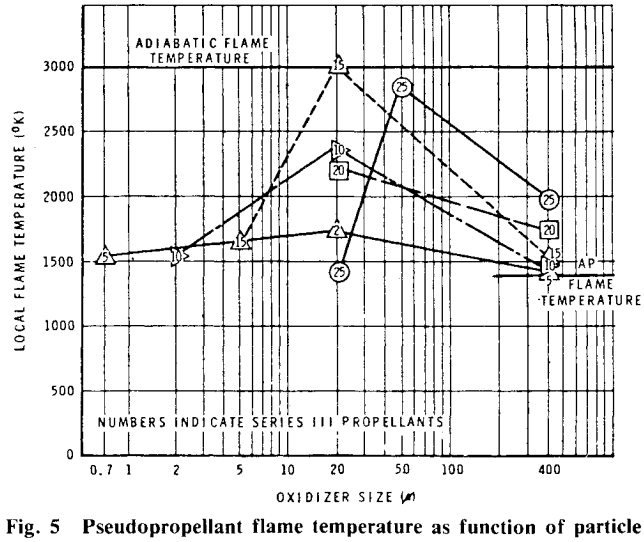

Fig. 5 Pseudopropellant flame temperature as function of particle size (from Ref. 10 as applied to Ref. 23 propellants, Ref. 23 numbering scheme indicated).

flame with the AP decomposition products, and there is experimental evidence for such interaction. Beckstead's solution, like Cohen's, is coupled but there are more terms to keep track of. Both have reported some difficulties with the iteration, which may be symptomatic of remaining inconsistencies. This is going to be a problem as the modeling gets more complicated, and merits careful attention.

Although the new versions are more physically appealing than the old ones, the violations of continuity continue to be disturbing. The Workshop[11] did not recommend forcing the decomposition rates to preserve the formulation. However, it may be necessary to provide additional terms or mechanisms to do so. It was recommended[11] that future work consider interactions between adjacent unlike particles. Cohen[11] has performed such an analysis whereby an interacting flame is added to the flame structure of a coarse particle adjacent to a fine particle. However, the work is not considered complete and has not been formally published.

Other Model Extensions

Aluminized Propellants

Cohen, Glick-Condon, and the old Beckstead version treat aluminum in a very simplified way. First its presence is accounted for in the computation of oxidizer volume fraction wherever that is used in the model. It is as though the binder were a higher density material. Second, the flame temperature used accounts for the thermochemistry of the aluminum. Thus the flame energy is increased. Third, a heat of fusion term is added to the energy balance since aluminum particles generally melt and agglomerate at the surface. The current Beckstead model is the first attempt to incorporate the details of aluminum behavior in a propellant combustion model. The model is described reasonably well in Ref. 10. Only a synopsis of what is done will be given here.

The aluminum occupies space as in the simple model. The heat of fusion term is added to the binder energy balance only, because the aluminum is in the binder. Rather than use a new thermochemical flame temperature to redefine Q_{PF} and Q_{FF}, new flame heat release terms are added to the oxidizer and binder energy balances. The other multiple flame thermochemistry remains as before, as though no aluminum were present. This approach is probably a better representation of how the aluminum contributes. The heat release terms are similar in form to those for the primary flame: there is a heat of reaction, an exponential in "flame height," and a proportioning of the heat feedback between oxidizer and binder surfaces. The aluminum weight fraction determines its contribution to the mass flow. The heat release terms represent a sum of contributions from "parent aluminum" (particles as formulated) and "agglomerated aluminum." The problem is to determine the fraction agglomerated, the agglomerate size, and the "flame height" for parent and agglomerated aluminum. The heat of reaction is a numerical constant which depends upon the oxidizer assumed (water appears to be the most realistic oxidizer in this context).

The fraction agglomerated is determined from a correlation of experimental data obtained for bimodal AP/HTPB propellants.[37] The correlation shows strong dependencies on the coarse AP size and the coarse/fine ratio, and a weak dependence on the aluminum size. Cohen has reviewed those data and disagrees with Beckstead's correlation because it omits important dependencies upon the fine AP size and pressure. Given the fraction agglomerated, the agglomerate size is determined from a pocket volume theory. The pocket volume is the volume in between coarse AP particles. The concept requires that the coarse AP particles be large compared to all the other particles; it breaks down as the number of aluminum particles per pocket approaches 1, and Beckstead tries to correct for that. Given the parent size and the agglomerate size, the flame height for each is determined by applying particle ignition and combustion theory in association with calculation of the respective particle motion. All particles are assumed to be spherical, which is a good representation of particles above the surface and of most particles at the surface. The ignition distance is that at which an ignition criterion is satisfied, and the combustion distance is the remaining distance in which the particle size goes to zero.

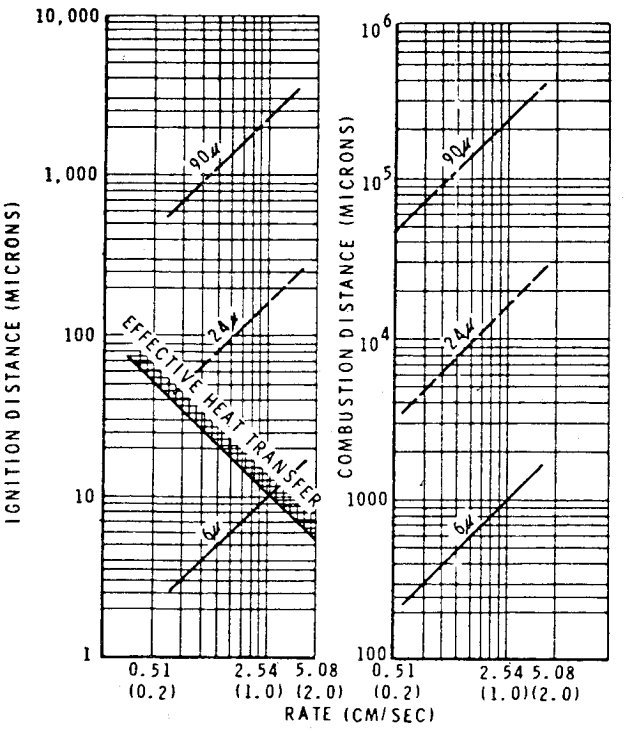

Fig. 6 Computed ignition and combustion distances of aluminum particles (from Ref. 10).

Some parametric results of ignition and combustion distances as functions of aluminum particle size and propellant burn rate are shown in Fig. 6. The essential point of this figure is that aluminum burning occurs too far away from the surface to contribute anything significant to the surface energy balance. An exception would be fine parent particles which do not agglomerate, but that is a contradiction because fine particles are found to agglomerate quite extensively. The distances are reasonable in light of what is observed from motion pictures of burning propellants.

The simple and sophisticated models, and data in general, indicate that aluminum per se has a small effect upon burning rate. For most practical propellants, the effect appears to be rather one of removing oxidizer or binder or both to make room for the aluminum. Exceptions may be explained by surface interaction effects which lower burn rate, or circumstances whereby there are many fine particles burning to raise burn rate. The former is not addressed at all in the model, and the latter would require a more refined description of the aluminum behavior. Beckstead has made use of existing knowledge in a tractable way, and it is a good step forward.

Catalyzed Propellants

The models treat catalysts by modifying one or more of the kinetics constants contained. An optimization or calibration is performed in association with burning rate data to try to deduce the principal parameter affected. In this way, the model can help to discern the catalytic mechanism. Once the effect is deduced, the calibrated model is presumably applicable to other propellants in that class. The models do not describe a mechanism of catalysis per se, and would not be able to predict the effect of some new additive a priori.

Using the BDP model, Cohen and Beckstead found that iron oxide could be described by increasing A_{ox}, the prefactor

of AP decomposition. Cohen increases A_{ox} by an order of magnitude for every percentage of iron oxide, and finds diminishing returns consistent with data. However, ferrocene compounds cannot be described that simply; both surface and gas phase processes appear to be affected, according to the model, but Cohen believes that changing the primary flame rate constant is the best single change that would describe the effect.

Beckstead[10] currently employs a modified rate constant expression based upon a heterogeneous adsorption mechanism which depends upon specific surface area. The expression used is given by Eq. (B-18). The particular k, A, E, and T subscript depends upon the particular step chosen. Beckstead now argues that iron oxide catalyzes the primary flame (k_{PF}) rather than the AP decomposition. Cohen disagrees, but there are supporting arguments for both sides. The expression requires two floating parameters, C_1 and C_2, which are calibrated by data. Glick-Condon[18,38] optimize the activation energy component of rate constant as a function of catalyst concentration and specific surface. It would be difficult to define the specific surface of active material produced by the decomposition of a liquid catalyst.

Nitramine Propellants

The only published model of nitramine propellants in the BDP framework is that of Cohen, Price, and Strand.[7,8] The model builds upon earlier BDP ideas[3,5] and later experimental work.[32,39] A modeling effort by Beckstead and McCarty is currently in progress, but has not yet been published.

The model modifications take note of the different surface and flame structures of nitramine propellants, and the different physical and chemical properties of nitramines, relative to AP propellants and AP. The nitramines of greatest interest are HMX and the very similar RDX. These nitramines are energetic monopropellants, and are fairly well balanced stoichiometrically such that they cannot really be called "oxidizers." Relative to AP, these nitramines have very low melting points and bulk melting of particles has been observed at low heating rates (low burning rates). Indeed, at conventional rocket pressures, the propellant surface is a planar melt consisting of the nitramine and binder which appears to have admixed with the nitramine at the particle peripheries.[3,32,39] At high pressure, above what has been identified as a particle size-dependent critical burn rate, the surface structure takes on a markedly different appearance.[32,39] Surface craters form, which are identified with combustion along paths of adjoining particles. It has been observed that, under these conditions, the nitramine particles are no longer melting. The flame structure consists of an active primary flame and the monopropellant flame. It is plausible that fuel binder decomposition products can react with some of the oxidizing species produced by nitramine decomposition to form a primary flame. However, a final flame is unlikely because there is nothing left to react the excess fuel. In the case of an active binder, even a primary flame is unlikely because both ingredients are stoichiometrically balanced and experiments have shown no interaction. Other physical, chemical, and thermochemical constants required by the model will change relative to AP propellants. Only a synopsis of Cohen's method will be given here.

New expressions for S_{ox}/S_o are employed to describe the planar and cratered surface states. For the planer state, it is the particle volume fraction corrected by a floating parameter to attempt to account for the peripheral binder interference. The floating parameter appears to have a conceptual error in that it implies more interference with coarse particles than with fine particles; further study or explanation is needed. For the cratered state, it is an exaggeration of the BDP model expression since h/D_o can exceed 1. It is not consistent as an expression of geometry, but it makes the essential point that S_{ox}/S_o approaches 1 so that the burning becomes dominated by the nitramine as shown by data. The change in the surface structure is deemed to occur at that burning rate (heating rate) where passage of the solid phase thermal wave across a spherical particle is too fast to heat the bulk particle to its melting point. The criterion is derived by a simple transient heating analysis of a spherical particle. The shift in the surface structure is the proposed mechanism for a major shift in pressure exponent observed with nitramine propellants.

The flame structure follows the BDP model, except that there is no final flame. Diffusion length floating parameters are adjusted from AP propellant values. For bimodal nitramine propellants calculated as $j=1$ (old version), b is computed using an average D' and δ. For $j=2$ (new version), each b is determined by δ and the respective D'. Unlike AP, it makes very little difference whether a bimodal propellant is calculated by the $j=1$ or $j=2$ method. These adjustments are in the nature of fine tuning because the diffusion flame is relatively unimportant. For nitramine propellants, the diffusion flame temperature is much lower than the monopropellant flame temperature; the reverse is true with AP. With active binder, the diffusion flame is omitted. The weak diffusion flame is the proposed explanation for the small effect of particle size on burning rate. The major role of particle size on burning rate is to locate the region of the exponent shift, and to that extent there is a major effect on burning rate over that region.

Results

Monomodal Propellants

The BDP model standard cases were three AP/polysulfide propellants. Two contained 70% AP, one of 20μ particle size and the other of 200μ. The third contained 60% of 20μ AP. The burning rate predictions were good for two of the cases, but on the low side for 200μ AP. Of equal importance, results for surface temperature, flame heights, surface structure, etc. (i.e., various internal details), were reasonable.

Glick-Condon[15] performed an interesting exercise on two of these cases to illustrate the individual effects of their proposed model modifications. Some of their results for one case are shown in Table 1 as the ratio of burning rate computed with the indicated modification to the BDP rate. The only significant change is by the use of time-averaging rather than the statistical average particle. But even here, the effect is limited principally to higher pressures and is not a large effect. Differences for the 200μ case were even smaller.

A comparison has also been made between the BDP model (as represented by Cohen[11]) and King's model. The comparison would reflect the combined effects of the most elaborate departures from BDP. King[19] used three AP/HTPB propellants containing 73% AP; particle sizes were 5μ, 20μ, and 200μ. Several important points were gleaned from this exercise, so it is shown as a busy Fig. 7. The striking observations are the gross underprediction of the 200μ case and the virtual identity of the two models for that case. Both models predict the other two cases reasonably well, but there are differences in the character of the curves produced. King's model is better as to general pressure exponent behavior, but BDP is better in picking up the inflection in slope which is attributed to the β_F shift (AP flame becoming controlling). King is able to improve his predictions as a whole by optimizing the kinetics of his subsurface reactions.[19] There is a large effect on the 200μ case, as shown, but only small effects on the other cases (not shown, in the interests of figure clarity). This is probably the most important point, and merits further discussion because it illustrates a latent deficiency in the BDP model.

Cohen's calculations showed that the β_F shift occurs at lower pressures as particle size increases. For 5μ, it occurred at about 100 atm (arguably in agreement with the data). For 20μ, it occurred at about 35 atm (in agreement with the data). For 200μ, according to the model, the β_F shift occurred below

Table 1 Effect of modifications to BDP model on computed burning rates for an AP/polysulfide propellant (70% AP, 20μ) (Ref. 15)

Pressure, atm.	Replace S_o with S_P(Eq. 1)	Eq. (B-6) for b	More terms in B-S series	Time-average method
3.5	1.000	0.991	1.000	0.981
6.3	1.006	0.988	1.006	0.976
11.2	1.004	0.972	1.004	0.943
20.0	1.003	0.953	1.006	0.896
35.3	1.005	0.934	1.007	0.852
63.4	1.046	0.964	1.014	0.796
112.3	1.074	0.966	1.034	0.728

10 atm. Thus the entire regime is one of AP flame control. Predictions are good in regimes of diffusion flame control, but become poor in regimes of AP flame control (coarse AP or high pressure). King's optimization served to magnify a pressure-dependent AP heat release process. It is very important where AP fully takes over from the diffusion flame as the primary energy source (200μ), but of little importance otherwise (5μ and 20μ). In the BDP model, there is no sustaining pressure-dependent heat release term in the regime of AP control. The AP flame approaches a collapsed flame asymptote ($\xi^*_{AP} \to 0$), which is reflected completely by the predicted burn rate curve for 200μ. Q_{ox} is not pressure-dependent in the BDP model, but effectively becomes so in King's model with optimized constants.

This "latent" deficiency has not been noted before because circumstances have not encountered it or have masked it. Higher flame temperatures, multimodal sizes, and a restricted upper pressure all will promote diffusion flame control through most of the calculations. All of the multimodal calculations to be presented have this latent deficiency, but it is "dormant" for these reasons. King has proposed a correction, but it is not necessarily accurate. The advanced monopropellant models[20] incorporate related, but better justified, mechanisms that would produce a similar effect. Miller[11] has argued that the final flame merits a reconsideration in the quantitative scheme, which could augment pressure-dependent heat feedback when $\beta_F < 1$. In any case, there is some unfinished business to resolve.

The final point to be gleaned from these exercises is that most of the BDP approximations have been vindicated. Certain elaborations which have more physical or intellectual appeal are going to cost computer program development and run times without appreciably changing the results. This is not a trivial matter as the extended modeling grows more complicated to address practical propellants.

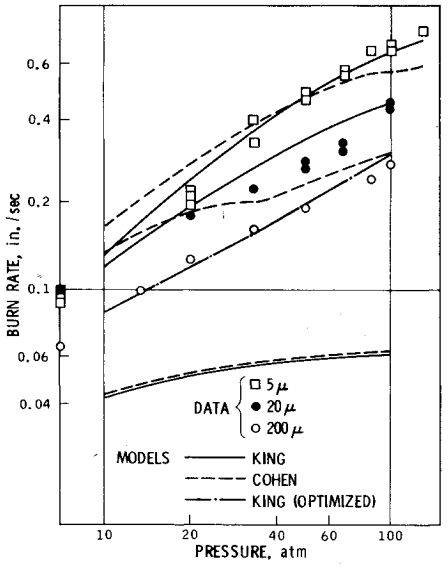

Fig. 7 Comparison of Cohen and King models for 73% AP (monomodal)/HTPB propellants.

Multimodal Propellants

Miller's statistical correlation of his data for trimodal AP propellants, by an effective average particle size, is shown in Fig. 8. This correlation may be compared with parametric model results for the effect of monomodal particle size on burning rate. The model results, for Glick-Condon and Beckstead calculations at Miller's solids loading, are shown in Fig. 9. Although the monomodal size cannot really be compared with the Miller average size, the ability of the models to show the qualitative mechanistic particle size effect is encouraging. Condon also shows the effect of particle size distribution width or standard deviation for polydisperse monomodal sizes. This detail is but a small correction to the monodisperse results. Consistent with remarks pertaining to Table 1, the time-averaging method departs from the BDP method results most significantly with finer sizes.

Another example of parametric results, for bimodal AP, is Beckstead's old version results shown in Fig. 10. Condon[36] has made the same calculations, and the results are quite

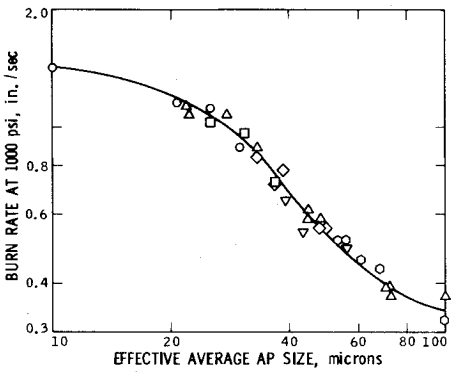

Fig. 8 Correlation of burn rate data by effective AP average particle size (from Ref. 23).

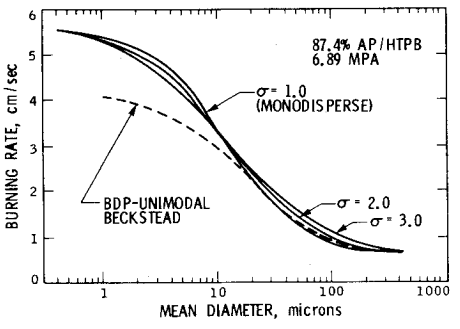

Fig. 9 Effect of monomodal AP size on burning rate, Beckstead (monodisperse) and Glick-Condon (polydisperse) models (from Ref. 36).

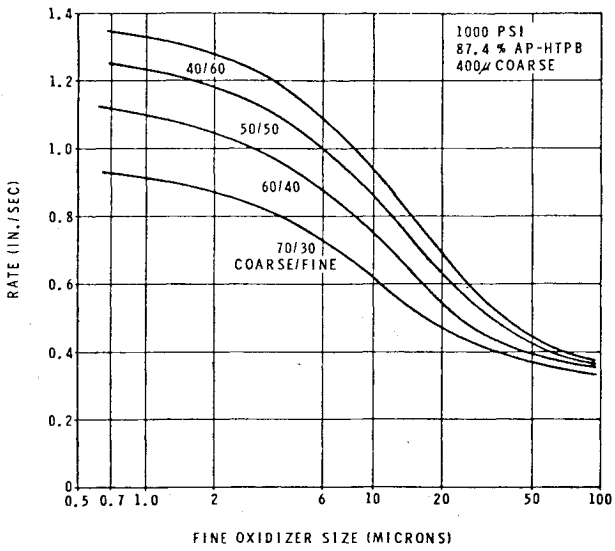

Fig. 10 Effect of bimodal AP distribution on burn rate, Beckstead model (from Ref. 9).

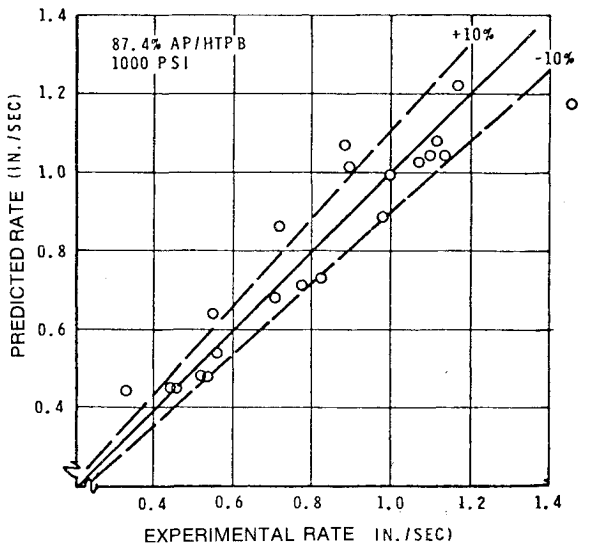

Fig. 12 Beckstead comparisons of theoretical and experimental burning rates, Ref. 23 trimodal propellants (from Ref. 9).

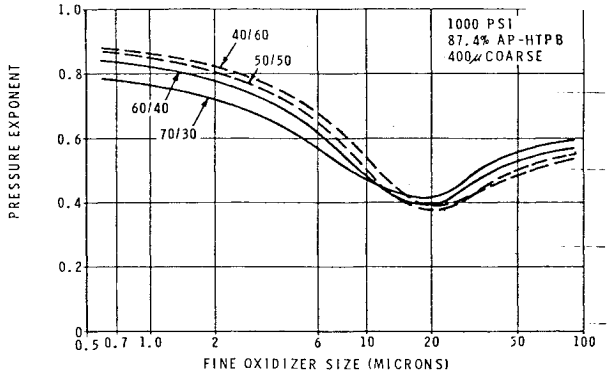

Fig. 11 Effect of bimodal AP distribution on pressure exponent, Beckstead model (from Ref. 9).

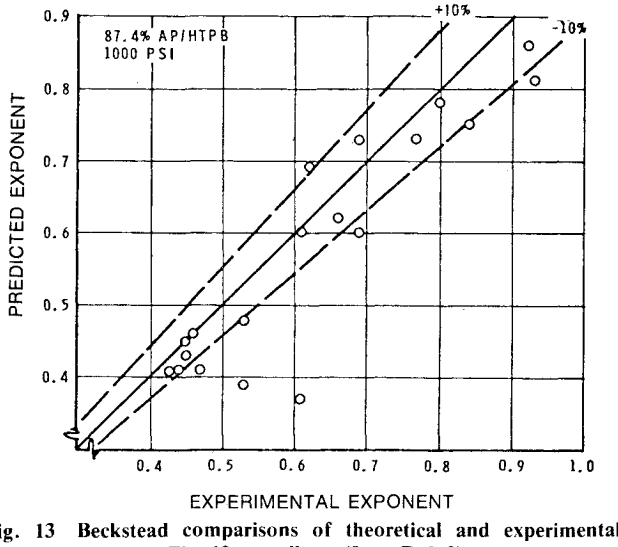

Fig. 13 Beckstead comparisons of theoretical and experimental pressure exponents, Fig. 12 propellants (from Ref. 9).

similar. These calculations typify what can be done with and learned from the models. Similar curves have been generated for pressure exponent and temperature sensitivity. Beckstead's pressure exponent results are shown in Fig. 11. Note that there is an optimum fine size, and a stronger effect of fine size than coarse/fine ratio. The trends are qualitatively correct. Figures 12 and 13 demonstrate a remarkable quantitative agreement with Miller's rate and exponent data, respectively. Condon[36] shows comparable agreement. It appears that multimodal propellants further wash out differences between time-averaged pseudopropellant and BDP-type approaches.

Beckstead and Glick-Condon have noted that, in general, agreement with data is worst where there is a large difference between coarse and fine sizes. Cohen[8] explored that point using the $j=1$ and $j=2$ capabilities of his model. Burning rate curves and data for three propellants studied are shown in Fig. 14. Where the two sizes were least different, the old version method ($j=1$) provided good agreement with data. However, agreement became poor for the propellant having the largest size difference. On the other hand, the $j=2$ method (two separate sets of flames and surface temperatures) provided good agreement for that case (as shown) but not for the other two (omitted for figure clarity). Cohen's interacting flame work is attempting to resolve this disparity, so that consistent results may be achieved with the preferred $j=2$ approach. Miller[11] has strongly endorsed the idea of interacting flame modeling because he sees particle size interactions running through his data correlations.[23]

Aluminized Propellants

Glick-Condon comparisons with some of Miller's aluminized propellant rate data are shown in Fig. 15. The Miller numbering scheme is included on the figure. The agreement is good for some propellants and bad for others. Beckstead[9] performed the same calculations with his old version model and showed similar discrepancies. A systematic problem appears to be those propellants having the widest spread between coarse and fine AP sizes in their respective subgroups. Those are the high points on Fig. 15. Thus aluminum interactions are affecting the AP particle size interactions to such a degree that the modeling must address them. Miller believes that the interplay is related to the near-surface flame chemistry. In that view, it is more a question of the assignment of oxidizing species in an interacting flame approach, rather than a better model of the aluminum behavior per se.

Historically, practical aluminized propellants did not contain such wide spreads in modal AP sizes. Thus earlier predictions[6] and developmental experience indicated small effects of aluminum, such that a simplified model could cope with it. Many of the Fig. 15 predictions are consistent with this background.

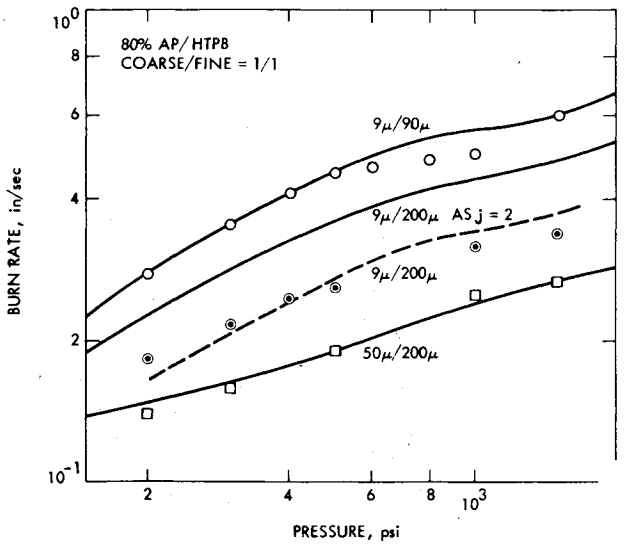

Fig. 14 Cohen-Price-Strand model comparisons with data for bimodal AP propellants, two model versions (from Ref. 8).

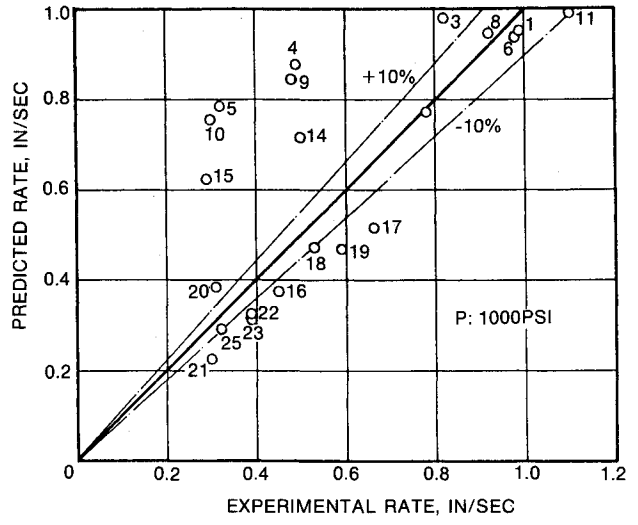

Fig. 15 Glick-Condon comparisons of theoretical and experimental burning rates, Ref. 23 aluminized propellants (from Ref. 38).

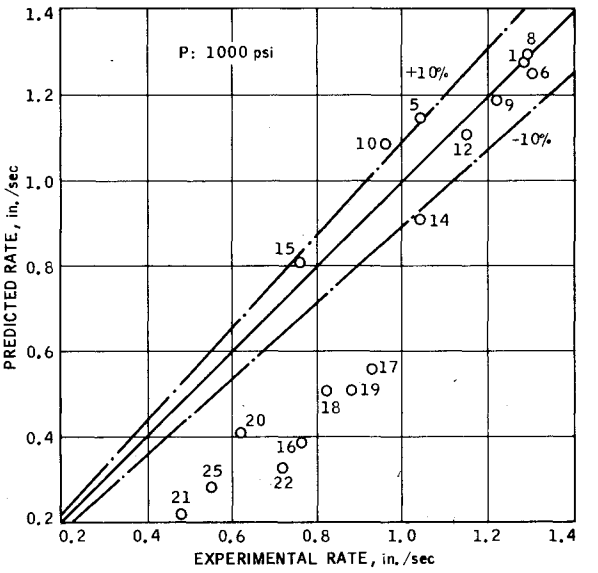

Fig. 16 Glick-Condon comparisons of theoretical and experimental burning rates, Ref. 23 catalyzed (iron oxide)-aluminized propellants (from Ref. 38).

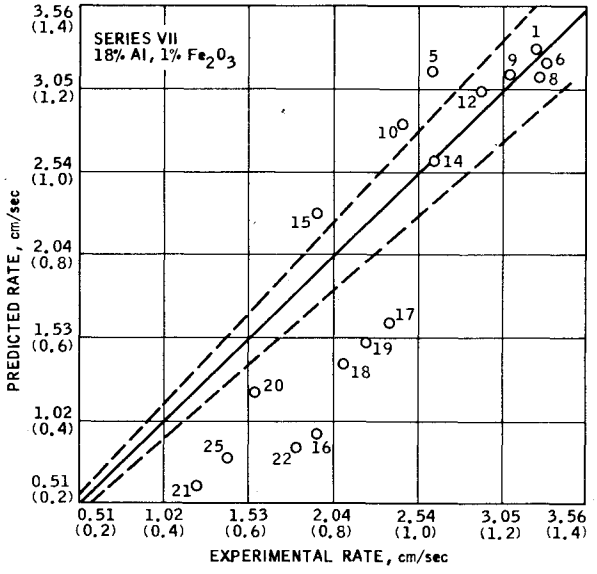

Fig. 17 Beckstead comparisons of theoretical and experimental burning rates, Fig. 16 propellants (from Ref. 10).

Catalyzed Propellants

Glick-Condon and Beckstead calculations for Miller's catalyzed aluminized propellants are compared with data in Figs. 16 and 17, respectively. The agreement is poor for lower burn rate propellants. The remarkable thing, however, is the comparison between the models themselves. Here are two different models being applied to many propellants containing trimodal AP, 18% aluminum, and 1% iron oxide, yet the two figures are nearly identical.

Miller[23] noted that the addition of iron oxide removed most of the interaction effects caused by the aluminum. Therefore, the predictions should have reverted back to the accuracy of Fig. 12. They did not, but rather show discrepancies which are qualitatively different from the Fig. 15 discrepancies. Thus it is concluded that the problem lies in the treatment of the catalytic effect. It has not been described or optimized correctly. Cohen would argue that, in the case of iron oxide, the change should be in the kinetics of AP decomposition rather than the primary flame.

Nitramine Propellants

Results for two HMX propellants are shown in Fig. 18. An attempt was made to approach monodisperse propellants by particle screening for each batch. Ordinarily, a given lot of HMX is quite polydisperse. The result, for the coarse HMX propellant, was a record-breaking exponent shift. The monodisperse model shows this as a discontinuity in the surface structure at the critical burn rate. The burn rate jumps to a value that is essentially the HMX rate. The slight exponent shift in the fine HMX propellant is the β_F shift. Rates do not jump as long as the surface remains planar. Approximately, the critical rate is inversely proportional to particle size. These data were used to calibrate the floating parameters in the model. Upon calibration, the model was successfully applied to other monomodal HMX and RDX propellants.[7]

The latent deficiency discussed earlier does not show up in the HMX propellant calculations. This is perhaps due to the different kinetics and energetics, etc., constants of HMX and HMX propellants. Nevertheless, corrections for AP propellants should be carried over to nitramine propellants to the extent relevant.

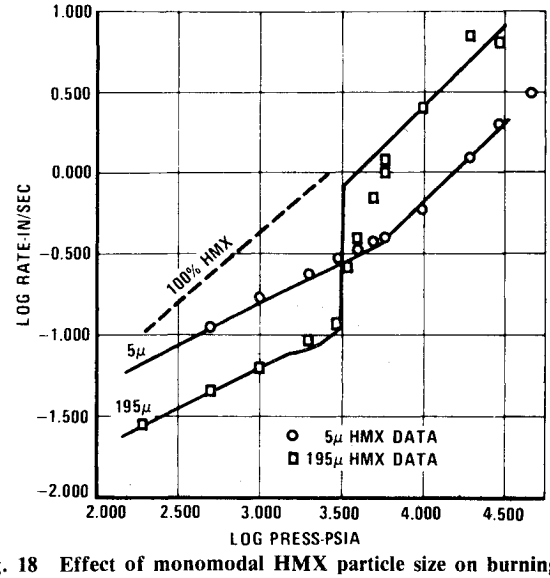

Fig. 18 Effect of monomodal HMX particle size on burning rate, 75% HMX/HTPB, Cohen-Price model and data (from Ref. 7).

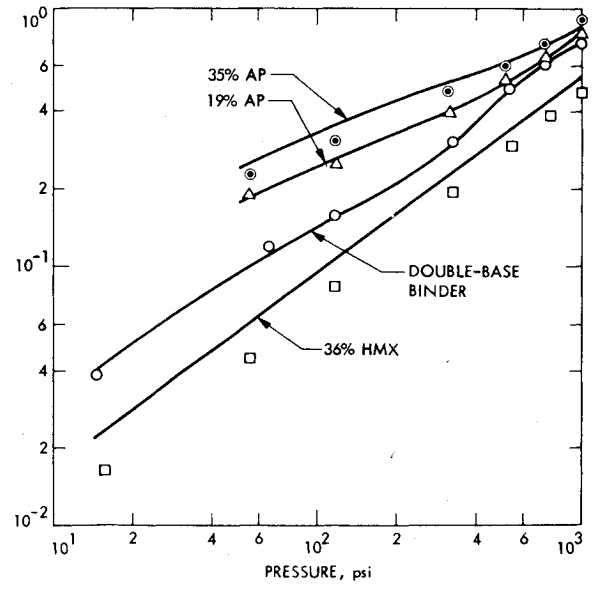

Fig. 20 Burning rates of AP and HMX active binder propellants, Cohen-Price-Strand model and data (from Ref. 8).

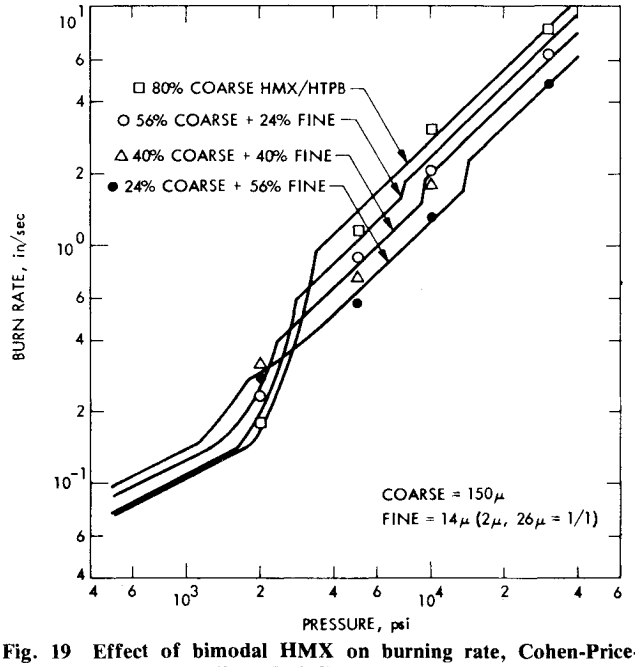

Fig. 19 Effect of bimodal HMX on burning rate, Cohen-Price-Strand model and data (from Ref. 8).

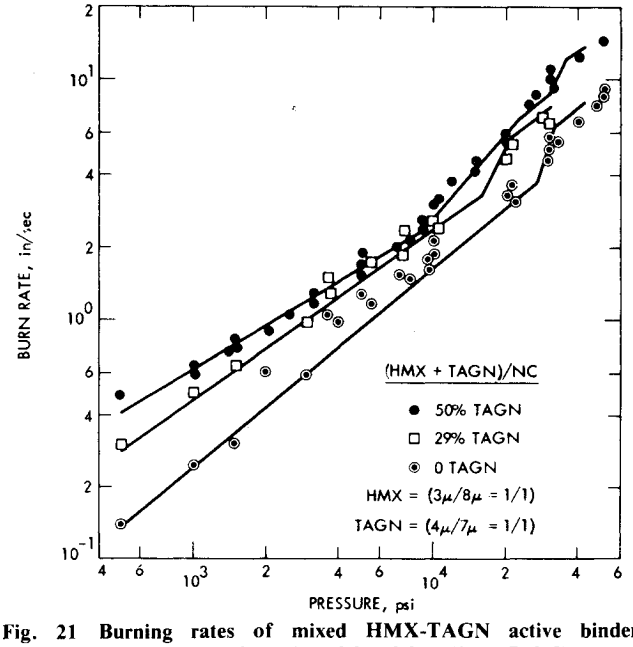

Fig. 21 Burning rates of mixed HMX-TAGN active binder propellants, Cohen-Price-Strand model and data (from Ref. 8).

Results for a series of bimodal HMX propellants are shown in Fig. 19. Based upon examination of fine HMX particle size distributions, Cohen has split the fine component into two sizes. He has made an issue of HMX particle size quality control in connection with the exponent shift and hazards problems. Thus the model has viewed these propellants as trimodal. Cohen and Price found that, for nitramine propellants, the $j=1$ and $j=2$ features of the model can be combined to calculate up to four particles. Although numerically unimportant, it is conceptually inconsistent. The predictions show the observed effect of changing coarse/fine ratio very well. The second small exponent shift, at high pressure, is due to the surface transition of the 26μ component size. Based upon model results, methods to avoid or mitigate exponent shifts have been proposed.[32]

Active Binder Propellants

The effects of adding AP or HMX to an energetic double-base binder are shown in Fig. 20. The key to these predictions is the treatment of the diffusion flame in Cohen's model. With AP, it is present such that the burning rate increases at low and intermediate pressures. The rate would also be noticeably particle-size dependent. The latent deficiency would not show up because the active binder takes over control at high pressures. With HMX, the diffusion flame is omitted such that the burning rate falls if the HMX rate is lower than the binder rate. The rate would not be noticeably particle-size dependent, except for exponent shift behavior at pressures higher than plotted here. The way the binder is treated in Cohen's model, the prediction for the binder alone is data-in, data-out. As noted before, there is a need to incorporate a combustion model for the binder. Beckstead has not as yet reported results of doing so.

Cohen-Price-Strand results for mixed oxidizer active binder propellants are shown in Fig. 21. TAGN (triaminoguanidine nitrate) is treated conceptually the same as HMX, but with appropriate changes in input constants (lower melting point, faster decomposition kinetics, etc.). For these calculations,

HMX corresponds to $j=1$ and TAGN to $j=2$. For each j, there are two i sizes having the same surface temperature. The binder here is single-base, less energetic than the Fig. 20 binder. The predictions are in good agreement with the data. In general, the model has been very satisfactory except for numerical instabilities sometimes encountered at an exponent shift.

Input Constants

Sets of values of input constants used in the respective models are reported in Refs. 4, 18, 19, and 32. Some of the inputs are properties which have not been measured, or which have controversial values. Unknown values have been derived by calculation or deduction, so are probably in error to some degree. Although the values appear to be reasonable and are given circumstantial support by the calculated results, the uncertainty imposes a limitation on the models.

Concluding Remarks

Composite propellant burn rate modeling has developed to a point where it can and does make useful contributions to combustion research and practical propellant development. The models are able, at least qualitatively, to explain the burning rate characteristics of a wide variety of propellants of interest. However, deficiencies do remain and there is work yet to be done in order to improve the quantitative aspects and predictive capability in general.

A judgment will not be made as to the "best" model or approach. There are many similarities and, where there are differences, each has its own virtues and faults. However, certain remarks can be made based upon the facts presented in this review. It does not appear necessary to go to the trouble of tracking and time-averaging individual particles. Nor does it seem necessary to detail the polydisperse nature of a given modal particle size. Nor does it seem necessary to solve the complete Burke-Schumann problem. On the other hand, apportionment of component masses and energies is necessary, provided that it is done carefully and properly, with conservation preserved and component interactions accounted for; otherwise, the attempt will lead to inconsistencies, poor results, and/or iteration problems. There is some housecleaning and restructuring to be done.

In moving forward, a list of priority items may be presented as follows: restoration of the proper pressure-dependence for AP propellants where $\beta_F << 1$, by incorporating an improved monopropellant combustion model or other justifiable mechanism; accounting for component interactions, first without aluminum, but especially with aluminum as an eventuality; re-examination of the role of the final flame for AP propellants; completing a model for the active binder; further study of the catalytic process; in a different vein, improvements in numerical methods to facilitate the coupled solution of multiple ingredients having separate surface temperatures; and last but not least, experimental work to obtain needed input values and improved understanding that would serve to replace floating parameters.

Appendix

Nomenclature

A = kinetics prefactor
A_{fh} = average flame height factor
b = characteristic diffusion flame dimension
c = a dimensionless characteristic length
c_p = propellant specific heat (c_g is for the gas)
C = various floating parameter constants
D_o = oxidizer particle size
D' = diameter intercepted by a plane through a sphere
D'_{PD} = adjusted value of D' in King's model
$\bar{D}_m$ = mean diameter of the mth mode
d = distance regressed from the top of an oxidizer particle
$\mathfrak{D}$ = diffusion coefficient
E = activation energy
F_{Di} = log normal distribution function
F_m = modal weight fraction of all modes
h = distance from planar surface to point of particle regression
$J( )$ = Bessel function
k = rate constant
m = mass flux
m_{ign} = power in particle ignition delay law
$\mathfrak{M}$ = molecular weight
O/F = local oxidizer/fuel ratio
P = pressure
Q = heat release
r = burning rate
$\bar{r}$ = time-averaged burning rate for tracking models
R = gas constant
S = surface area
S_{oxAP} = portion of AP surface assigned to $HClO_4$ that consumes NH_3
t = time
T = temperature
u_{ign} = power in particle ignition delay law
v = gas velocity
x^* = flame height
Y = mole fraction in decomposition products
α = weight fraction of ingredient in propellant
α^* = weight fraction in pseudopropellant
β = fraction of reactants
γ = fraction of energy from primary flame that heats oxidizer
δ = interstitial spacing
δ = with a subscript, reaction order
η = Burke-Schumann dimensionless height above surface
η' = lumped parameter, Eq. (B-7a)
ϕ_i = root of Bessel function
Φ = stoichiometric oxidizer/fuel ratio
Φ_M = stoichiometric molar oxidizer/fuel ratio
λ = thermal conductivity
ν = ratio of stoichiometric oxidizer/fuel ratio to local oxidizer/fuel ratio
ψ = dimensionless characteristic length, Eq. (GC-7d)
ρ = density
σ_m = modal standard deviation of size distribution
ξ = Burke-Schumann dimensionless radial position
ξ^* = dimensionless flame height
ζ = volume fraction of ingredient in propellant
ζ^* = volume fraction in pseudopropellant

Subscripts

AP = associated with oxidizer monopropellant flame
AP′ = effective value at monopropellant flame
c = catalyst
D = associated with final flame
DB = double-base binder
f = binder, or referring to binder characteristics
F = associated with diffusion flame
FF = associated with final flame
i = ith particle size
j = jth oxidizer (or particle size when calculating separate surface temperatures)
m = associated with melting (or mth mode)

o	= initial condition (or total surface)
ox	= oxidizer, or referring to oxidizer surface characteristics
p	= propellant as a whole
P	= planar
PD,PF,PDF	= associated with primary flame (diffusion, reaction, total)
s	= surface
ss	= associated with subsurface reactions
T	= total
v	= associated with a vaporization process
fPF	= example of combined subscript: fraction of binder associated with primary flame reaction

Numbering system includes initials of modelers (B—Beckstead, C—Cohen, GC—Glick-Condon, K—King); no initial denotes common usage.

Continuity Relations (Eqs. 1)

$$m_T S_o = r\rho_p S_o = m_{ox} S_{ox}/\alpha_{ox} \tag{C-1}$$

$$m_T S_P = r\rho_p S_P = m_{ox} S_{ox}/\alpha_{ox} \tag{GC-1}$$

$$m_T S_o = r\rho_p S_o = m_{ox} S_{ox} + m_f S_f \tag{B-1}$$

$$m_T S_P = r(\rho_p S_P = m_{ox} S_{ox} + m_f S_f) \tag{K-1}$$

$$\bar{r} = \Sigma(m_T \Delta t)/(\rho_p \Sigma \Delta t) \tag{GC-1a}$$

$$\bar{r} = [\Sigma(m_{ox} S_{ox} + m_f S_f)]/(\rho_p \Sigma S_P) \tag{K-1a}$$

Ingredient Decomposition (Eqs. 2)

$$m_{ox} = \rho_{ox} r_{ox} = A_{ox} e^{-E_{ox}/RT_s} \tag{2a}$$

$$m_f = \rho_f r_f = A_f e^{-E_f/RT_s} \tag{2b}$$

Surface Area Relations (Eqs. 3-5)

$$\frac{S_{ox}}{S_o} = \frac{\zeta_{ox}\left[3\left(\frac{h}{D_o}\right)_P^2 + 3\left(\frac{h}{D_o}\right)_N^2 + 1\right]}{1 + \zeta_{ox}\left[3\left(\frac{h}{D_o}\right)_P^2 + 3\left(\frac{h}{D_o}\right)_N^2\right]} \tag{B-3, C-3}$$

$$\left(\frac{h}{D_o}\right)_{P/N} = \frac{1}{2}\left(1 \pm \frac{1}{\sqrt{3}}\right)\left(1 - \frac{r_{ox}}{r_f}\right) + r_{ox}\frac{t_{ign}}{D_o} \tag{B-4, C-4}$$

$$\frac{S_{ox}}{S_P} = \frac{S_{ox}}{S_o}\frac{S_o}{S_P} = \frac{h^2 + (D'/2)^2}{(D'/2)^2(1/\zeta_{ox})} \tag{GC-3}$$

$$\frac{S_{ox}}{S_P} = \frac{h^2 + (D'/2)^2}{S_P(\zeta_{ox}, D_o, d_f)} \tag{K-3}$$

$$D' = 2(d_f D_o - d_f^2)^{1/2} \tag{GC,K-3a}$$

$$h = d_{ox} - d_f \tag{GC,K-4}$$

$$d_{ox} = \begin{cases} 0 & (t \le t_{ign}) \\ \Sigma(m_{ox}\Delta t)/\rho_{ox} \end{cases} \tag{GC,K-4a}$$

$$d_f = \Sigma(m_f \Delta t)/\rho_f \tag{GC,K-4b}$$

$$t_{ign} = C_{ign} D_o^{u_{ign}+1}/P^{m_{ign}} \tag{B,C,GC-5}$$

Characteristic Surface Dimensions (Eqs. 6)

$$b = \frac{D_o}{\sqrt{6}}\left(1 + \sqrt{\frac{3}{2}}\frac{\delta}{D_o}\right) \tag{C-6}$$

$$\frac{\delta}{D_o} = \left(\frac{\pi}{6\zeta_{ox}}\right)^{1/3} - \sqrt{\frac{2}{3}} \tag{C-6a}$$

$$b = \frac{D'}{2\sqrt{\zeta_{ox}}} \tag{GC-6}$$

$$b = D_o/\sqrt{6\zeta_{ox}} \tag{B-6}$$

$$b = \sqrt{S_P/\pi} \tag{K-6}$$

$$D'_{PD} = \frac{b}{\left(1 + \frac{m_f S_f}{m_{ox} S_{ox}}\frac{\mathfrak{M}_{ox}}{\mathfrak{M}_f}\right)^{1/2}} \tag{K-6a}$$

Flame Heights (Eqs. 7-11)

$$x^*_{PD} = A_{fh} C_{PD} \eta' b/\phi_1 \tag{B-7}$$

$$x^*_{PD} = A_{fh} C_{PD} b/(\eta' \phi_1) \tag{C-7}$$

$$\eta' = \ell n\left[\frac{2(1+\nu)cJ_1(c\phi_1)}{(\nu - (1+\nu)c^2)\phi_1 J_o^2(\phi_1)}\right] \tag{B-7a, C-7a}$$

$$x^*_{PD} = A_{fh}\eta b/\psi \tag{GC-7}$$

$$x^*_{PD} = \eta b/\psi \tag{K-7}$$

where η must satisfy Eq. (GC, K-7a).

$$\frac{\nu - (1+\nu)c^2}{2(1+\nu)c} = \sum_1^\infty \frac{J_1(c\phi_i)}{\left\{\begin{matrix} J_o^2(\phi_i) \\ \text{or} \\ J_o(\phi_i) \end{matrix}\right\}} J_o(\phi_i \xi)$$

$$\times \exp\left[-\frac{(1+4\psi^2\phi_i^2)^{1/2} - 1}{2\psi^2}\eta\right] \tag{GC-7a, K-7a}$$

$$c = D'/2b \tag{B,C,GC-7b}$$

$$c = D'_{PD}/2b \tag{K-7b}$$

$$\nu = \Phi(1 - \alpha_{ox})/\alpha_{ox} \tag{B,C,GC-7c}$$

$$\nu = \Phi_M \frac{Y_f(1 - Y_{fss})}{Y_{ox}(1 - Y_{oxss})}\left[\left(\frac{b}{D'_{PD}}\right)^2 - 1\right] \tag{K-7c}$$

$$\psi = (\mathfrak{D}/v)b \tag{GC,K-7d}$$

$$\mathfrak{D}/v = \frac{\mathfrak{D}_o T_s^{1.75}\mathfrak{M}_p}{RT_s m_T} \tag{GC-7e}$$

$$\mathfrak{D}/v = \frac{\mathfrak{D}_o T_s^{1.5}\mathfrak{M}_{ox}}{RT_s m_{ox}}\frac{\pi D'^2_{PD}}{S_{ox}} \tag{K-7e}$$

$$x^*_{PF} = \frac{(1+\nu)^2}{\nu}\frac{RT_s}{\mathfrak{M}_{ox}}T_F^2\frac{S_{ox}}{\pi D'^2_{PD}}\frac{m_{ox}}{k_{PF}P^{\delta_{PF}}} \tag{K-8}$$

$$x^*_{PF} = m_T/(k_{PF}P^{\delta_{PF}}) \tag{B,C,GC-8}$$

$$k_{PF} = A_{PF} e^{-E_{PF}/RT_F} \tag{8a}$$

$$x^*_{AP} = \frac{RT_s}{\mathfrak{M}_{ox}} \frac{S_{ox}}{\pi D'^2_{PD}} \frac{m_{ox}}{k_{AP} P^{\delta_{AP}}} \quad \text{(K-9)}$$

$$x^*_{AP} = m_{ox}/(k_{AP} P^{\delta_{AP}}) \quad \text{(B,C,GC-9)}$$

$$k_{AP} = A_{AP} e^{-E_{AP}/RT_{AP}} \quad \text{(9a)}$$

$$x^*_{FF} = x^*_{AP} + x^*_D \quad \text{(B,C,GC-10)}$$

$$\xi^* = m c_g x^*/\lambda \quad \text{(11)}$$

Energy Balance (Eqs. 12-13)

$$m_T c_p (T_s - T_o) = -\alpha_{ox} m_T Q_{ox} - \alpha_f m_T Q_f + \beta_F m_T Q_{PF} e^{-\xi^*_{DF}} + (1-\beta_F)\alpha_{ox} m_T [Q_{AP} e^{-\xi^*_{AP}} + Q_{FF} e^{-\xi^*_{FF}}] \quad \text{(C,GC-12)}$$

$$m_T c_p (T_s - T_o) = -\alpha_{ox} m_T Q_{ox} - \alpha_f m_T Q_f + \beta_F m_T Q_{PF} e^{-\xi^*_{DF}} + (1-\beta_F)\alpha_{ox} m_T Q'_{AP} e^{-\xi^*_{AP}} \quad \text{(B-12)}$$

$$m_T c_p (T_s - T_o) = -m_{ox} \frac{S_{ox}}{S_p} [\beta_{oxss} Q_{ox} + (1-\beta_{oxss}) Q_{vox} + Q_{mox}] - m_f \frac{S_f}{S_P} [(1-\beta_{fss}) Q_{vf} + Q_{mf}] + m_T c_p (T_F - T_S) \frac{e^{\xi^*_D} - 1}{\xi^*_{PD} e^{\xi^*_{DF}} - (e^{\xi^*_D} - 1)} + m_T \frac{S_{oxP}}{S_P} Q_{AP} (1-\beta_{oxss})(1-\beta_F) \frac{\xi^*_{PD} e^{(\xi^*_{DF} - \xi^*_{AP})} - (e^{\xi^*_D} - 1)}{\xi^*_{PD} e^{\xi^*_{DF}} - (e^{\xi^*_D} - 1)} \quad \text{(K-12)}$$

$$Q_{AP} = c_p (T_{AP} - T_o) + Q_{ox} \quad \text{(B,C,GC-12a)}$$

$$Q_{PF} = c_p (T_F - T_o) + \alpha_{ox} Q_{ox} + \alpha_f Q_f \quad \text{(B,C,GC-12b)}$$

$$\alpha_{ox} Q_{FF} = c_p (T_F - T_o) - \alpha_{ox} c_p (T_{AP} - T_o) + \alpha_f Q_f \quad \text{(B,C,GC-12c)}$$

$$T'_{AP} = T_F - \frac{Q_{FF}}{c_p} [1 - e^{-(\xi^*_{FF} - \xi^*_{AP})}] \quad \text{(B-9b) (GC-9b)}$$

$$\beta_F = \frac{x^*_{AP} - x^*_{PF}}{x^*_{PD}} A_{fh} \quad \text{(B,C,GC-13)}$$

Model Extensions (Eqs. 14-18)

$$\bar{r} = \sum_j \frac{1}{\rho_{oxj}} \left[\sum_m \left(\sum_i \frac{\overline{m}_{Ti}}{\zeta^*_{oxi}} F_{Di} \Delta D_i \right)_m F_m \right]_j \quad \text{(GC-14)}$$

$$F_{Di} = \frac{1}{\sqrt{2\pi}\sigma_m} \exp\left[-\frac{1}{2} \left(\frac{\ln D_i - \ln \overline{D}_m}{\sigma_m} \right)^2 \right] \quad \text{(GC-14a)}$$

$$m_T = \sum \frac{S_{oxj}}{m_{oxj} s_o} + \left(1 - \sum \frac{S_{oxj}}{S_o}\right) \rho_f r_f \quad \text{(C-14)}$$

$$m_T = \sum m_{oxj} \frac{S_{oxj}}{S_o} + m_f \frac{S_f}{S_o} \quad \text{(B-14)}$$

$$\zeta^*_{oxj} = \left[1 + \frac{\zeta_f / D_j}{\Sigma (\zeta_{oxj}/D_j)} \right]^{-1} \quad \text{(B-15)}$$

$$\zeta^*_{oxi} = \left[1 + \frac{D_i^{\zeta N-3} \zeta_f}{\Sigma D_i^{\zeta N-3} \zeta_{oxi}} \right]^{-1} \quad \text{(GC-15)}$$

$$\frac{(m_{ox}S_{ox})_j}{\Sigma (m_{ox}S_{ox})_j} m_T c_p (T_{sj} - T_o) = -\frac{(m_{ox}S_{ox})_j}{S_o} Q_{oxj} - \left[m_T - \Sigma \frac{(m_{ox}S_{ox})_j}{S_o} \right] \frac{(m_{ox}S_{ox})_j}{\Sigma (m_{ox}S_{ox})_j} Q_f + \frac{(m_{ox}S_{ox})_j}{S_o} (1-\beta_{Fj}) [Q_{APj} e^{-\xi^*_{APj}} + Q_{FFj} e^{-\xi^*_{FFj}}] + \frac{(m_{ox}S_{ox})_j}{\Sigma (m_{ox}S_{ox})_j} m_T \beta_{Fj} Q_{PFj} e^{-\xi^*_{DFj}} \quad \text{(C-16)}$$

$$T_{soxj} = T_o - \frac{Q_{oxj}}{c_p} + \gamma_j \beta_{Fj} \left(1 + \frac{1}{(O/F)_j}\right) \times \frac{Q_{PFj}}{c_p} e^{-\xi^*_{DFj}} + (1-\beta_{Fj}) \frac{Q'_{APj}}{c_p} e^{-\xi^*_{APj}} \quad \text{(B-16)}$$

$$Q'_{APj} = Q_{APj} + \left[(1-\beta_{Fj}) \left(1 + \frac{1}{(O/F)_j}\right) - \beta_{APj} \right] Q_{FF} e^{-(\xi^*_{FFj} - \xi^*_{APj})} \quad \text{(B-16a)}$$

$$(O/F)_j = \frac{(m_{ox}S_{ox})_j}{(m_f S_f)_j} = \frac{D_j}{\alpha_f} \sum \frac{\alpha_{oxj}}{D_j} \quad \text{(B-16b)}$$

$$\beta_{APj} = \frac{(m_{ox}S_{oxAP})_j}{(m_{ox}S_{ox})_j} = 0.34 \text{ (chemistry)} \quad \text{(B-16c)}$$

$$\beta_{Fj} = \frac{(m_f S_{fPF})_j}{(m_f S_f)_j} = \frac{(m_{ox}S_{oxPF})_j}{(m_{ox}S_{ox})_j} = \text{Eq. (13)} \quad \text{(B-16d)}$$

$$\gamma_j = 2/3 \quad \text{(assumed)} \quad \text{(B-16e)}$$

$$T_{sf} = T_o - \frac{Q_f}{c_p} + \sum \left[(1-\gamma_j) \beta_{Fj} \frac{\alpha_{oxj}}{\alpha_f} \left(1 + \frac{1}{(O/F)_j}\right) \frac{Q_{PFj}}{c_p} \times e^{-\xi^*_{DFj}} \right] + \beta_{DB} \frac{Q_{DB}}{c_p} e^{-\xi^*_{DB}} \quad \text{(B-17)}$$

$$\beta_{DB} = 1 - \frac{\Sigma (m_f S_{fPF})_j}{m_f S_f} = 1 - \sum \frac{\beta_{Fj}}{(O/F)_j} \frac{\alpha_{oxj}}{\alpha_f} \quad \text{(B-17a)}$$

$$k = A e^{-E/RT} P^2 \left(1 + \frac{\alpha_c S_c}{C_1 + \alpha_c S_c} \frac{C_2}{A} \frac{1}{P}\right) \quad \text{(B-18)}$$

Acknowledgment

Support for this review was provided in part by the AFOSR through NASA and the Jet Propulsion Laboratory, and in part by Norman Cohen Professional Services. The author acknowledges the cooperation of M.W. Beckstead, R.L. Glick, and M.K. King in answering many questions regarding their models. The Appendix fulfills an action item of the 1978 JANNAF Workshop on Burn Rate Modeling. The paper was prepared at the invitation of the AIAA.

References

[1] Hermance, C.E., "A Model of Composite Propellant Combustion Including Surface Heterogeneity and Heat Generation," *AIAA Journal,* Vol. 4, Sept. 1966, pp. 1629-1637.

[2] Hermance, C.E., "A Detailed Model of the Combustion of Composite Solid Propellants," *Proceedings of the AIAA/ICRPG Second Solid Propulsion Conference,* June 1967, pp. 89-103.

[3] Derr, R.L., Beckstead, M.W., and Cohen, N.S., "Combustion Tailoring Criteria for Solid Propellants," AFRPL-TR-69-190, Lockheed Propulsion Co., May 1969.

[4] Beckstead, M.W., Derr, R.L., and Price, C.F., "A Model of Composite Solid Propellant Combustion Based on Multiple Flames," *AIAA Journal,* Vol. 8, Dec. 1970, pp. 2200-2207.

[5] Beckstead, M.W., Derr, R.L., and Price, C.F., "The Combustion of Solid Monopropellants and Composite Propellants," *Thirteenth Symposium (International) on Combustion,* Combustion Institute, Pittsburgh, Pa., 1971, pp. 1047-1056.

[6] Cohen, N.S., Derr, R.L., and Price, C.F., "Extended Model of Solid Propellant Combustion Based on Multiple Flames," *Proceedings of 9th JANNAF Combustion Meeting,* CPIA Publication 231, Vol. II, Dec. 1972, pp. 25-42.

[7] Cohen, N.S. and Price, C.F., "Combustion of Nitramine Propellants," *Journal of Spacecraft and Rockets,* Vol. 12, Oct. 1975, pp. 608-612.

[8] Cohen, N.S., Price, C.F., and Strand, L.D., "Analytical Model of the Combustion of Multicomponent Solid Propellants," AIAA Paper 77-927, July 1977.

[9] Beckstead, M.W., "Combustion Calculations for Composite Solid Propellants," *Proceedings of 13th JANNAF Combustion Meeting,* CPIA Publication 281, Vol. II, Dec. 1976, pp. 299-312.

[10] Beckstead, M.W., "A Model for Solid Propellant Combustion," *Proceedings of 14th JANNAF Combustion Meeting,* CPIA Publication 292, Vol. I, Dec. 1977, pp. 281-306.

[11] Roe, W.E., 1978 JANNAF Workshop on Burn Rate Modeling, Lancaster, Calif., April 1978.

[12] Glick, R.L., "Statistical Analysis of Non-Metallized Composite Solid Propellant Combustion," *Proceedings of 10th JANNAF Combustion Meeting,* CPIA Publication 243, Vol I, Dec. 1973, pp. 157-184.

[13] Glick, R.L., "On Statistical Analysis of Composite Solid Propellant Combustion," *AIAA Journal,* Vol 12, March 1974, pp. 384-385.

[14] Glick, R.L., "Steady-State Combustion of Non-Metallized Composite Solid Propellants," Report U-75-27, Thiokol Corp., Huntsville, Ala., July 1975.

[15] Glick, R.L. and Condon, J.A., "Statistical Analysis of Polydisperse, Heterogeneous Propellant Combustion: Steady-State," *Proceedings of 13th JANNAF Combustion Meeting,* CPIA Publication 281, Vol. II, Dec. 1976, pp. 313-345.

[16] Glick, R.L., "Distribution Functions for Statistical Analysis of Monodisperse Solid Propellant Combustion," *AIAA Journal,* Vol. 14, Nov. 1976, pp. 1631-1633.

[17] Miller, R.R., Hartman, K.O., and Myers, R.B., "Prediction of Ammonium Perchlorate Particle Size Effect on Composite Propellant Burning Rate," *Proceedings of 26th JANNAF Solid Propulsion Meeting,* CPIA Publication 196, Vol. I, May 1970, pp. 567-591.

[18] Condon, J.A. and Osborn, J.R., "The Effect of Oxidizer Particle Size Distribution on the Steady and Nonsteady Combustion of Composite Propellants," AFRPL-TR-78-17, Purdue University, School of Mechanical Engineering, West Lafayette, Ind., June 1978.

[19] King, M.K., "Model for Steady State Combustion of Unimodal Composite Solid Propellants," AIAA Paper 78-216, Jan. 1978.

[20] Price, C., Boggs, T., and Derr, R., "Modeling of Solid Monopropellant Deflagration," AIAA Paper 78-219, Jan. 1978.

[21] BenReuven, M., Caveny L.H., Vichnevetsky, R. and Summerfield, M., "Flame Zone and Subsurface Reaction Model for Deflagrating RDX," *Sixteenth Symposium (International) on Combustion,* Combustion Institute, Pittsburgh, Pa., 1977, pp. 1223-1233.

[22] Miller, R.R., Donohue, M.T., and Peterson, J.P., "Ammonium Perchlorate Size Effects on Burn Rate—Possible Modification by Binder Type," *Proceedings of 12th JANNAF Combustion Meeting,* CPIA Publication 273, Vol. II, Dec. 1975, pp. 371-388.

[23] Miller, R.R., Donohue, M.T., Yount, R.A. and Martin, J.R., "Control of Solids Distribution in HTPB Propellants," AFRPL-TR-78-14, Hercules Inc., Allegheny Ballistics Laboratory, Cumberland, Md., April 1978.

[24] Flanagan, J.E. and Oberg, C.L., "A Modified Two-Stage Flame Model of Steady-State Composite Solid Propellant Combustion," Report 59-017, Rocketdyne Div., Rockwell/International Corp., Canoga Park, Calif., Sept. 1970.

[25] Sammons, G.D., "Solid Propellant Combustion Modeling," *Proceedings of 10th JANNAF Combustion Meeting,* CPIA Publication 243, Vol. I, Dec. 1973, pp. 149-156.

[26] Sammons, G.D., "Scientific Report: Multiple Flame Combustion Model Fortran IV Computer Program," Report R-4827, Rocketdyne Div., Rockwell/International Corp., March 1974.

[27] Strahle, W.C., "Some Statistical Considerations in the Burning of Composite Propellants," *AIAA Journal,* Vol. 16, Aug. 1978, pp. 843-847.

[28] Blum, E.H. and Wilhelm, R.H., "A Statistical Geometric Approach to Random-Packed Beds," *AIChE-Industrial Chemical Engineering Symposium Series,* No. 4, London Institute of Chemical Engineers, 1965 pp. 4:21-4:27.

[29] King, M.K., "An Analytical and Experimental Study of the Erosive Burning of Composite Propellants," Part A, AFOSR-TR-78-0060, Atlantic Research Corp., alexandria, Va., Nov. 1977.

[30] Burke, S.P. and Schumann, T.E.W., "Diffusion Flames," *Ind. and Eng. Chem.,* Vol. 20, Oct. 1928; see also *First and Second Symposium on Combustion,* Combustion Institute, Pittsburgh, Pa., 1965., pp. 2-11.

[31] Williams, F.A., *Combustion Theory,* Addison-Wesley, Boston, 1965, pp. 37-45.

[32] Cohen, N.S. and Strand, L.D., "Nitramine Propellant Research," AFOSR-TR-76-1163, NASA TM-33-801, Jet Propulsion Labaratory, Pasadena, Calif., Oct. 1976.

[33] King, M.K., "An Analytical and Experimental Study of the Erosive Burning of Composite Propellants [etc.]," Report TR-PL-5763, Atlantic Research Corp., Alexandria, Va., Nov. 1976.

[34] Cohen, N.S. and Bowyer, J.M., "Combustion Response Modeling for Composite Solid Propellants," AFRPL-TR-78-39, Jet Propulsion Laboratory, Pasadena, Calif., June 1978.

[35] Beckstead, M.W. and McCarty, K.P., "Calculated Combustion Characteristics of Nitramine Monopropellants," *Proceedings of 13th JANNAF Combustion Meeting,* CPIA Publication 281, Vol. II, Dec. 1976, pp. 57-68.

[36] Renie, J.P., Condon, J.A., and Osborn, J.R., "Oxidizer Size Distribution Effects," *Proceedings of 14th JANNAF Combustion Meeting,* CPIA Publication 292, Vol. I, Dec. 1977, pp. 325-339.

[37] Micheli, P.L. and Schmidt, W.G., "Behavior of Aluminum in Solid Rocket Motors," AFRPL-TR-77-29, Vol. I, Aerojet Solid Propulsion Co., Sacramento, Calif., Dec. 1977.

[38] Glick, R.L. and Condon, J.A., "Statistical Combustion Modeling—The Effect of Additives," *Proceedings of 14th JANNAF Combustion Meeting,* CPIA Publication 292, Vol. I, Dec. 1977, pp. 341-378.

[39] Cohen N.S., "Combustion of Nitramine Propellants," *Proceedings of 11th JANNAF Combustion Meeting,* CPIA Publication 261, Vol. I, Dec. 1974, pp. 267-283.